# Quantized point vortex equilibria in a one-way interaction model with a Liouville-type background vorticity on a curved torus

Takashi Sakajo[1] and Vikas S. Krishnamurthy[2]

[1)] *Department of Mathematics, Kyoto University, Kitashirakawa Oiwake-cho, Kyoto 606-8502, JAPAN*

[2)] *Faculty of Mathematics, University of Vienna, Oskar-Morgenstern-Platz 1, 1090 Vienna, Austria*

(*sakajo@math.kyoto-u.ac.jp)

(Dated: 3 April 2022)

We construct point vortex equilibria with strengths quantized by multiples of $2\pi$ in a fixed background vorticity field on the surface of a curved torus. The background vorticity consists of two terms, first a term exponentially related to the stream function, and a second term arising from the curvature of the torus, which leads to a Liouville-type equation for the stream function. By using a stereographic projection of the torus onto an annulus in a complex plane, the Liouville-type equation admits a class of exact solutions given in terms of a loxodromic function on the annulus. We show that appropriate choices of the loxodromic function in the solution leads to stationary vortex patterns with $4\widehat{n}$ point vortices of identical strengths, $\widehat{n} \in \mathbb{N}$. The quantized point vortices are stationary in the sense that they are equilibria of a 'one-way interaction' model where the evolution of point vortices is subject to the continuous background vorticity, while the background vorticity distribution is not affected by the velocity field induced by the point vortices. By choosing loxodromic functions continuously dependent on a parameter and taking appropriate limits with respect this parameter, we show that there are solutions with inhomogeneous point vortex strengths, in which the exponential part of the background vorticity disappears. The point vortices are always located at the innermost and outermost rings of the torus owing to the curvature effects. The topological features of the streamlines are found to change as the modulus of the torus changes.

## I. INTRODUCTION

Formation of a vortex-like tube having its circulation quantized by the Planck constant $\hbar$ in superfluid helium was theoretically predicted by Feynman (1955). This prediction was confirmed later in a laboratory experiment of a rotating superfluid (two-dimensional) thin film by Yarmchuk, Gordon, and Packard (1979), who found identical vortex-like cores organized in polygonal patterns. More recently many lattice patterns of quantized vortices have been observed in Bose–Einstein condensates (BECs) (Abo-Shaeer *et al.*, 2001; Engels *et al.*, 2002, 2003). Abrisokov, in his Nobel lecture (Abrikosov, 2004), suggested *vortex lattice theory* as a theoretical model for investigating such quantized vortex patterns. Suppose that the velocity field in the azimuthal direction induced by a localized vortex core depends only on the distance $s$ from the core and its magnitude decays as $1/s$ for $s \gg 1$. Vortex lattice patterns are then characterized by equilibrium states of vortex cores under their mutual interaction through the induced velocity field. Although it is a simple phenomenological model, the theoretical treatment of this model is much easier than that of physical models based on partial differential equations such as the Gross–Pitaevskii equation and the Ginzburg–Landau equation.

If we assume that the vorticity in the vortex core is concentrated at a discrete point, i.e., Dirac's $\delta$-measure, then the vortex lattice is equivalent to a system of $n$ point vortices with the circulation around a core corresponding to the strength of the point vortex there. The $n$-vortex problem has been utilized as a theoretical model to describe the equilibria and dynamics of vortices in the literature of hydrodynamics. See the book by Newton (2001) and the review article by Newton and Chamoun (2009) for references. Stationary lattice patterns formed by point vortices are referred to as *vortex crystals* (Aref *et al.*, 2003), whose investigation originated in the theory of vortex atoms due to Thomson in the 19th century. When we use vortex crystals as a model for vortex lattice patterns in superfluids and BECs, the strengths of the point vortices must be quantized. This means that the ratios of the strengths of all point vortex pairs must be integers. This is an important condition, since it is in contrast to the vortex motion of hydrodynamics in which the strengths of point vortices can be chosen to be arbitrary real numbers. It is known that vortex crystals with the same strength in the plane tend to acquire a certain symmetry, but, in general, vortex crystals in an asymmetric configuration do not usually have quantized strengths. In addition, most of the vortex crystals obtained so far are *relative equilibria* that translate or rotate at a constant speed without changing their relative configuration. To study vortex lattice patterns, we need to obtain fixed (or stationary) equilibria where all of the point vortices remain completely stationary. However, lesser number of fixed equilibria are known than relative equilibria.

Vortex crystals can also be considered on two-dimensional Riemannian manifolds. Vortex dynamics on a sphere (Newton, 2001) is well-studied due to its geophysical relevance. Kimura (1999) considered vortex dynamics on surfaces of constant curvature, including the sphere $S^2$ and a hyperbolic sphere $H^2$. The review by Turner, Vitelli, and Nelson (2010) discusses the general significance of vortices on surfaces with a non-constant Gaussian curvature and the effects of the non-constant curvature on the vortex dynamics. We are interested in how the non-constant curvature and the handle structure of a torus affect vortex crystal patterns on the torus. On a compact surface like a torus, just like on a sphere, the condition that the total vorticity needs to vanish has to be satisfied. Sakajo (2019b) formulated a numerical method to find vortex crystals on a torus, and found that the sum of the vortex circulations does not vanish in general for such crystals. This means that a constant background vorticity needs to be added in order for the total vorticity to vanish. Sakajo (2019b) further found that, in general, the point vortex strengths are not quantized when the background vorticity is constant. In order to overcome these difficulties and obtain vortex crystals with quantized strengths, in this paper we introduce a non-constant background vorticity distribution, given by a modified Liouville equation on the torus.

Consider that the stream function $\psi$ and the vorticity $\Omega$ associated with an incompressible velocity field in $\mathbb{R}^2$ satisfy $\Omega = -c\mathrm{e}^{d\psi}$ for $c, d \in \mathbb{R}$ with $cd < 0$. Without loss of generality, we take $c = 1$ and $d = -2$ so that $cd = -2$. Since $\Omega = -\nabla^2\psi$, where $\nabla^2$ is the planar Laplacian operator, this results in the planar Liouville equation

$$\nabla^2\psi = \mathrm{e}^{-2\psi} \tag{1}$$

for the stream function $\psi$. In the vorticity-stream function formulation of ideal fluid flow in $\mathbb{R}^2$, solutions to (1) also provide steady solutions of the Euler equation (Majda and Bertozzi, 2001). This is because the vorticity equation in this case reads $\Omega_t + \mathscr{J}(\Omega, \psi) = 0$, where $\mathscr{J}$ is the Jacobian, and any vorticity functional of the form $\Omega = V(\psi)$, where $V$ is a differentiable function, solves this vorticity equation. Furthermore, the Liouville equation is a fundamental nonlinear elliptic partial differential equation that appears in field theory and plasma physics. Mathematically, an important class of exact solutions to the planar Liouville equation are known (Bhutani, Moussa, and Vijayakumar, 1994; Calogero and Degasperis, 1982), and Crowdy (1997) has obtained the most general form of these solutions.

Vortex solutions of the Liouville equation have been studied in a variety of contexts. For example, see Horváthy and Yéra (1998); Akerblom *et al.* (2011) for a discussion in the context of field theory. In the context of hydrodynamics, Stuart (1967) constructed singly-periodic, everywhere smooth solutions to (1) that he used to model planar shear flows. Crowdy (2003) constructed solutions with a single point vortex surrounded by polygonal patterns of smooth vortices. Such solutions have been described as forming a "rational necklace" due to the rational functions appearing in the theory (Tur and Yanovsky, 2004; Tur, Yanovsky, and Kulik, 2011). Krishnamurthy *et al.* (2019) constructed exact solutions with two embedded point vortices in stationary equilibrium with the background vorticity term $-\mathrm{e}^{-2\psi}$. Indefinitely iterated solutions called "Liouville chains," containing increasing numbers of embedded point vortices in each iteration, have been constructed recently by Krishnamurthy *et al.* (2021), see Krishnamurthy *et al.* (2020) for the closely-related 'pure' point vortex equilibria which are limiting solutions in which the background vorticity vanishes.

The class of exact solutions to (1) can be written as

$$\psi(\zeta,\overline{\zeta}) = -\log\left[\frac{|f'(\zeta)|}{1+|f(\zeta)|^2}\right]. \tag{2}$$

This formula is given in terms of an arbitrary complex-valued analytic function $f(\zeta)$ and its derivative $f'(\zeta)$, with various choices of this function allowing us to construct many exact solutions in the complex $\zeta$-plane in a systematic manner. If the analytic function $f(\zeta)$ is chosen so that $f'(\zeta)$ has zeros at points $\zeta = v_k \in \mathbb{C}$, $k = 1,\dots,n$, then the stream function (2) has logarithmic singularities at each of the points $v_k$. These logarithmic singularities represent embedded point vortices in the flow. For $n$ point vortices with strengths $\Gamma_k \in \mathbb{R}$, $k = 1,\dots,n$, embedded in the background vorticity given by $-\mathrm{e}^{-2\psi}$, we are in fact solving the Liouville-type equation

$$\nabla^2\psi = \mathrm{e}^{-2\psi} - \sum_{k=1}^{n} \Gamma_k \delta_{v_k}. \tag{3}$$

To show that a solution $\psi$ of (3) is a stationary solution, it is necessary and sufficient to confirm that the point vortices in (3) remain stationary under the interaction with the other point vortices and the Liouville-type background vorticity field.

When we construct solutions to the Liouville-type equation on a torus based on the analytic formula (2), the equation (1) needs to be modified by adding a term corresponding to the curvature on the right hand side (Sakajo (2019a)):

$$\nabla^2_{\mathbb{T}_\alpha}\psi = \mathrm{e}^{-2\psi} - \kappa(\mathbb{T}_\alpha). \tag{4}$$

Here, $\mathbb{T}_\alpha$ is the torus with aspect ratio $\alpha$, $\nabla^2_{\mathbb{T}_\alpha}$ is the Laplace-Beltrami operator on $\mathbb{T}_\alpha$, and $\kappa(\mathbb{T}_\alpha)$ is the non-constant Gaussian curvature of $\mathbb{T}_\alpha$. The vorticity and stream function on $\mathbb{T}_\alpha$ are related by $\Omega = -\nabla^2_{\mathbb{T}_\alpha}\psi$. This class of exact solutions is found by the same method as in Crowdy (2004) who constructed solutions to a modified Liouville equation on the unit sphere. The class of solutions on the torus described by Sakajo (2019a) are smooth solutions except for two point vortices of equal strengths embedded at the two antipodal points.

As discussed in the planar case, when there are $n$ point vortices on the torus, we have the following modified Liouville equation for the stream function:

$$\nabla^2_{\mathbb{T}_\alpha}\psi = \mathrm{e}^{-2\psi} - \kappa(\mathbb{T}_\alpha) - \sum_{j=1}^{n} \Gamma_j \delta_{v_j}. \tag{5}$$

By recasting the Euler equation on a torus as a vorticity equation in the vorticity-stream function formulation, it can be shown that this vorticity equation has the important Jacobian term $\mathscr{J}(\Omega,\psi)$. The vorticity $\Omega = -\mathrm{e}^{-2\psi} + \kappa(\mathbb{T}_\alpha) + \sum_{j=1}^{n}\Gamma_j\delta_{v_j}$ is not a functional of $\psi$, because of the non-constant Gaussian curvature $\kappa(\mathbb{T}_\alpha)$. This implies that solutions of (5) are not, in general, solutions of the Euler equation on $\mathbb{T}_\alpha$. However, the solutions of the Liouville equation (5) can still be regarded as stationary configurations of quantized point vortices, in the following sense. We adopt (5) as a kinematic 'one-way interaction' model of localized vortex structures in superfluids and BECs. This means that the evolution of point vortices is subject to the continuous background vorticity, whilst the background vorticity distribution is not affected by the velocity field induced by the point vortices. This is the same situation as in the study of point vortex dynamics on a rotating sphere as considered by Newton and Shokraneh (2005), who introduce a one-way model in which point vortices are advected by the fixed continuous vorticity field corresponding to the solid body rotation of the sphere. In contrast to such a one-way interaction model, we can consider a 'two-way interaction' model where the background also evolves under the velocity field induced by the point vortices. The relation between the solutions of the Liouville equation and those of the Euler equation is further discussed in §VI.

The purpose of the present paper is to create a catalog of stationary lattice patterns of quantized point vortices embedded in background vorticity of Liouville-type on the surface of a curved torus. Since the toroidal surface is the simplest model of porous media having one handle structure, it is of theoretical significance to consider the formation of vortex lattice patterns in superfluid thin film as discussed by Corrada-Emmanuel (1994) and Machta and Guyer (1988). The exact solution gives rise to various quantized point vortices by specifying loxodromic functions that are doubly periodic in an annulus in the complex domain. The locations of quantized point vortices corresponds to zeros and poles of the loxodromic functions. To show that these quantized point vortices form a fixed equilibrium, we need to confirm two conditions. First is the Gauss condition, which requires that the total vorticity vanish on the toroidal surface. The second is a stationary condition, where the velocity field induced by point vortices and the Liouville-type background vorticity vanishes at the location of each quantized point vortex.

This paper is organized as follows. In Section 2, we review the exact solution of the modified Liouville equation on the surface of a curved torus given by Sakajo (2019a). We then provide the two conditions to be confirmed. In Section 3, we show the existence of stationary lattice patterns consisting of quantized point vortices with the choice of Weierstrass $\wp$-function. In Section 4, we obtain a continuous parametric family of stationary quantized point vortices when a loxodromic function is considered. After deriving a new solution formula of the modified Liouville equation, we construct another series of lattice pattern of quantized vortices in Section 5, called 'limit solutions'. The last section is summary and discussion for future studies.

## II. LIOUVILLE-TYPE EQUATION ON THE TOROIDAL SURFACE AND POINT VORTEX EQUILIBRIA

The geometry of a toroidal surface is generally characterized by the major radius $R$ and the minor radius $r$ with $R > r$. However, by its scale invariance, it is sufficient to deal with a canonical one, say $\mathbb{T}_\alpha$, with modulus $\alpha = R/r > 1$ in this paper. With the toroidal coordinates $(\theta, \phi) \in (\mathbb{R}/2\pi\mathbb{Z}) \times (\mathbb{R}/2\pi\mathbb{Z})$, it is embedded in the three-dimensional Euclidean space $\mathbb{E}^3$, which is represented by

$$(\theta, \phi) \mapsto ((\alpha - \cos\theta)\cos\phi, (\alpha - \cos\theta)\sin\phi, \sin\theta) \in \mathbb{E}^3. \tag{6}$$

Equation (4) is Liouville-type quasi-linear elliptic equation with respect to a scalar function $\psi(\theta, \phi)$ on the torus. The Laplace-Beltrami operator $\nabla^2_{\mathbb{T}_\alpha}$ and the Gauss curvature of the toroidal surface $\kappa(\mathbb{T}_\alpha)$, are respectively represented by

$$\nabla^2_{\mathbb{T}_\alpha} \equiv \frac{1}{(\alpha - \cos\theta)} \frac{\partial}{\partial\theta}\left((\alpha - \cos\theta)\frac{\partial}{\partial\theta}\right) + \frac{1}{(\alpha - \cos\theta)^2}\frac{\partial^2}{\partial\phi^2},$$
$$\kappa(\mathbb{T}_\alpha) \equiv -\frac{\cos\theta}{\alpha - \cos\theta}.$$

We also introduce a complex structure on the surface through a stereographic projection from the torus $\mathbb{T}_\alpha$ to the annulus $\{D_\zeta : \rho < |\zeta| \leq 1\}$ in a complex $\zeta$-plane as shown in figure 1. This

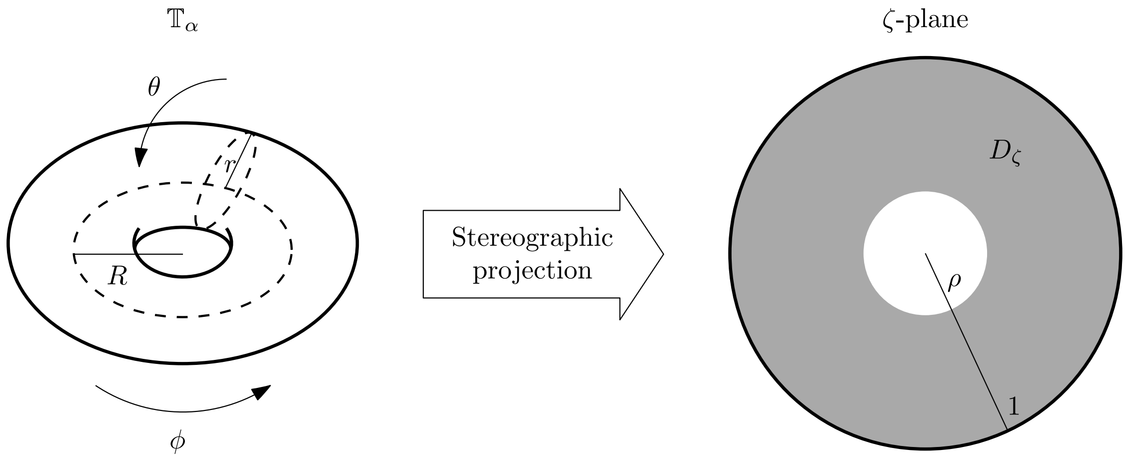


FIG. 1. Stereographic projection of the torus $\mathbb{T}_\alpha$, $\alpha = R/r > 1$, on the annulus $\{D_\zeta \mid \rho < |\zeta| \leq 1\}$. The toroidal angle $\phi \in [0, 2\pi)$ and the poloidal angle $\theta \in [0, 2\pi)$ are related to $\zeta$ through (7). Due to symmetry, the lower half of the torus (*viz.* $(\theta, \phi) = [0, \pi) \times [0, 2\pi)$) is mapped to $\sqrt{\rho} < |\zeta| \leq 1$ whereas the upper half of the torus (*viz.* $(\theta, \phi) = [\pi, 2\pi) \times [0, 2\pi)$) is mapped to $\rho < |\zeta| \leq \sqrt{\rho}$. The identity of $\theta = 0$ and $\theta = 2\pi$ corresponds to the identity of $|\zeta| = 1$ and $|\zeta| = \rho$.

stereographic projection is defined by

$$\zeta(\theta, \phi) = \mathrm{e}^{\mathrm{i}\phi} \exp(r_c(\theta)) \in \mathbb{C}, \qquad r_c(\theta) = -\int_0^\theta \frac{\mathrm{d}\hat{\theta}}{\alpha - \cos\hat{\theta}}. \tag{7}$$

The function $r_c(\theta)$ is monotonically decreasing owing to $r_c'(\theta) < 0$ for $1 < \alpha$, and satisfies the following quasi periodicity (Sakajo and Shimizu, 2016):

$$r_c(\theta \pm 2\pi) = \mp 2\pi\mathscr{A} + r_c(\theta), \qquad \mathscr{A} = (\alpha^2 - 1)^{-\frac{1}{2}}.$$

For later use, we evaluate $r_c(\theta)$ over the interval $[0, 2\pi)$:

$$r_c(0) = 0, \qquad r_c(\theta) = 2\mathscr{A} \tan^{-1}\left[\mathscr{B} \cot\left(\frac{\theta}{2}\right)\right] - \pi\mathscr{A} \quad \text{for } \theta \neq 0, \tag{8}$$

where $\mathscr{B} = \sqrt{\frac{\alpha-1}{\alpha+1}}$. The parameter $\rho$ associated with the conformal structure is related to the modulus $\alpha$ via the equation $\rho = \exp(-2\pi\mathscr{A}) = \exp(-2\pi/\sqrt{\alpha^2 - 1})$. Under the stereographic projection (7), $\theta = 0$ is mapped to the circle $|\zeta| = 1$, $\theta = 2\pi$ is mapped to the circle $|\zeta| = \rho$ and for $-\log\rho < r_c(\theta) \leq 0$ the torus is mapped to the annulus $\rho < |\zeta| \leq 1$. In particular, $\theta = \pi$ is mapped to the circle $|\zeta| = \sqrt{\rho}$. The periodicity of the torus in $\theta$ is thus transferred to the periodicity in $\rho$ on the $\zeta$-plane.

When the solution of (4) is regarded as the stream function, it gives rise to the incompressible velocity field on the toroidal surface: Suppose that a passive particle at $(\theta(t),\phi(t))$ on the toroidal surface at time $t$ is advected by the velocity field induced by the stream function $\psi$. Then, its governing equation is described by

$$\frac{\mathrm{d}\overline{\zeta}}{\mathrm{d}t} = -2\mathrm{i}\lambda^{-2}(\zeta,\overline{\zeta})\frac{\partial\psi}{\partial\zeta} \tag{9}$$

in the complex form (Sakajo and Shimizu, 2016). Here, $\overline{\zeta}$ is the conjugate of $\zeta$, and $\lambda(\zeta,\overline{\zeta})$ is the conformal factor associated with the metric $g$ on the toroidal surface (Green and Marshall, 2013), which is given by

$$\lambda(\zeta,\overline{\zeta}) = \frac{\alpha-\cos\theta}{|\zeta|}. \tag{10}$$

Based on (9), we rewrite the angular velocity fields on the toroidal surface in the $\theta$-direction as well as the $\phi$-direction explicitly. Substituting (7) and (10) into (9), we have

$$\frac{\mathrm{d}}{\mathrm{d}t}\left[\mathrm{e}^{-\mathrm{i}\phi(t)}\exp(r_c(\theta(t)))\right] = -\mathrm{i}\overline{\zeta}\frac{\mathrm{d}\phi}{\mathrm{d}t} - \frac{\overline{\zeta}}{\alpha-\cos\theta}\frac{\mathrm{d}\theta}{\mathrm{d}t} = -2\mathrm{i}\frac{|\zeta|^2}{(\alpha-\cos\theta)^2}\frac{\partial\psi}{\partial\zeta},$$

which yields

$$\frac{\mathrm{i}}{\alpha-\cos\theta}\frac{\mathrm{d}\theta}{\mathrm{d}t} - \frac{\mathrm{d}\phi}{\mathrm{d}t} = -\frac{2}{(\alpha-\cos\theta)^2}\zeta\frac{\partial\psi}{\partial\zeta}. \tag{11}$$

This indicates that the passive particle is at rest if $\zeta\frac{\partial\psi}{\partial\zeta}=0$. On the other hand, it follows from

$$\left.\frac{\partial}{\partial\theta}\right|_{\phi} = -\frac{\zeta}{\alpha-\cos\theta}\frac{\partial}{\partial\zeta} - \frac{\overline{\zeta}}{\alpha-\cos\theta}\frac{\partial}{\partial\overline{\zeta}}, \qquad \left.\frac{\partial}{\partial\phi}\right|_{\theta} = \mathrm{i}\zeta\frac{\partial}{\partial\zeta} - \mathrm{i}\overline{\zeta}\frac{\partial}{\partial\overline{\zeta}}$$

that

$$\zeta\frac{\partial}{\partial\zeta} = -\frac{\alpha-\cos\theta}{2}\frac{\partial}{\partial\theta} - \frac{\mathrm{i}}{2}\frac{\partial}{\partial\phi} \tag{12}$$

and thus we have

$$-\frac{\mathrm{i}}{\alpha-\cos\theta}\frac{\mathrm{d}\theta}{\mathrm{d}t} + \frac{\mathrm{d}\phi}{\mathrm{d}t} = \frac{2}{(\alpha-\cos\theta)^2}\left(-\frac{\alpha-\cos\theta}{2}\frac{\partial\psi}{\partial\theta} - \frac{\mathrm{i}}{2}\frac{\partial\psi}{\partial\phi}\right).$$

Accordingly, the angular velocity $u_\theta$ in the $\theta$-direction and $u_\phi$ in the $\phi$-direction of the toroidal surface $\mathbb{T}_\alpha$ is given by

$$u_\theta \equiv \frac{\mathrm{d}\theta}{\mathrm{d}t} = \frac{1}{\alpha-\cos\theta}\frac{\partial\psi}{\partial\phi}, \qquad u_\phi \equiv (\alpha-\cos\theta)\frac{\mathrm{d}\phi}{\mathrm{d}t} = -\frac{\partial\psi}{\partial\theta}, \tag{13}$$

which is a divergence-free vector field on $\mathbb{T}_\alpha$. Introducing the vorticity $\Omega$ as the curl of the velocity field (13), we obtain the elliptic equation $\nabla^2_{\mathbb{T}_\alpha}\psi = -\Omega$, in which the vorticity distribution is given by

$$-\Omega = \mathrm{e}^{-2\psi} - \kappa(\mathbb{T}_\alpha). \tag{14}$$

The analytic solution of the equation (4) has been provided explicitly in Sakajo (2019a):

$$\psi(\zeta,\overline{\zeta}) = -\frac{1}{2}\log\left[\frac{4|f'(\zeta)|^2}{(1+|f(\zeta)|^2)^2}\right] - \frac{1}{2}\log\left[\frac{|\zeta|^2}{(\alpha-\cos\theta)^2}\right], \tag{15}$$

in which $f(\zeta)$ is a given analytic function on a domain $D_\zeta$. The second term originates from the conformal factor, representing the curvature effect of the toroidal surface. It is regular, since we consider the function $f(\zeta)$ the domain $D_\zeta = \{\zeta \in \mathbb{C}\,|\,\rho < |\zeta| \leqq 1\}$ in the present paper. The first term is coming from the general solution to the Liouville equation in the plane (Liouville, 1853; Stuart, 1967). Crowdy (2004) has made two remarks on the nature of the analytic function $f(\zeta)$ so that the first term becomes non-singular. First, $f(\zeta)$ is not necessarily analytic everywhere in $D_\zeta$ and it can admit the finite number of simple poles in $D_\zeta$. Second, $f'(\zeta) \neq 0$ everywhere in $D_\zeta$. Additionally, in order to define the solution on the toroidal surface, the function is required to be doubly periodic in the domain $D_\zeta$.

As a matter of fact, as is discussed in Krishnamurthy *et al.* (2019, 2021), even if we allow the existence of simple zeros in $f'(\zeta)$ and double poles in $f(\zeta)$, one can still define the stream function (15) as a physical solution. Suppose that $f'(\zeta)$ has a simple zero or $f(\zeta)$ has a double pole at $\zeta = \nu_0$. Then the solution has the local behaviour,

$$\psi(\zeta,\overline{\zeta}) \sim -\log|\zeta-\nu_0| + \text{regular}, \qquad \zeta \to \nu_0.$$

On the other hand, the stream function of a point vortex located at $\zeta = \nu_0$ with the strength (circulation) $\Gamma$ on the toroidal surface has the following asymptotic expansion (Sakajo and Shimizu, 2016):

$$\psi(\zeta,\overline{\zeta}) \sim -\frac{\Gamma}{2\pi}\log\widehat{d}(\zeta,\nu_0) = -\frac{\Gamma}{2\pi}\log|\zeta-\nu_0| + \text{regular}, \qquad \zeta \to \nu_0, \tag{16}$$

in which the geodesic distance $\widehat{d}(\zeta,\nu_0)$ between $\zeta$ and $\nu_0$ is asymptotically represented by

$$\widehat{d}(\zeta,\nu_0) = \lambda(\nu_0,\bar{\nu}_0)|\zeta-\nu_0| + o(\zeta-\nu_0), \qquad \zeta \to \nu_0.$$

This indicates that the stream function (15) contains a point vortex at $\zeta = \nu_0$ with the strength $\Gamma = 2\pi$. Hence, when there exist $n$ simple zeros of $f'(\zeta)$ and double poles of $f(\zeta)$, say $\nu_j$, $j = 1,2,\ldots,n$, the solution contains $n$ point vortices at $\nu_j$ with the same strength $\Gamma_j = 2\pi$ in a field of Liouville-type vorticity distribution (14) on $\mathbb{T}_\alpha$. The vorticity distribution is thus given by

$$-\Omega = \mathrm{e}^{-2\psi} - \kappa(\mathbb{T}_\alpha) - \sum_{j=1}^{n}\Gamma_j\delta_{\nu_j}, \tag{17}$$

where $\delta_{v_j}$ denotes the $\delta$-measure at $v_j$. In this paper, we consider exact solutions to the modified Liouville equation (5) which corresponds to the vorticity distribution given by (17).

It is important to notice that the strengths of the point vortices are identical to $2\pi$. That is to say, the solution is regarded as the configuration of *quantized point vortices* on the surface of a torus in the background Liouville-type vorticity distribution. Such a stream function with point vortex singularities on the toroidal surface has already been obtained in Sakajo (2019a), in which $f(\zeta) = \mathrm{sn}(\log\zeta)/\mathrm{cn}(\log\zeta)$ with the Jacobi's elliptic functions $\mathrm{sn}(z)$ and $\mathrm{cn}(z)$ is chosen. The stream function yields stationary configuration of identical point vortices located at two antipodals of the toroidal surface, since $f'(\zeta)$ has two simple zeros in the fundamental domain.

Since $\mathbb{T}_\alpha$ is a compact surface without boundary, Gauss's divergence theorem gives rise to a global constraint on the vorticity distribution

$$\iint_{\mathbb{T}_\alpha} \Omega\,\mathrm{d}\sigma = 0, \tag{18}$$

in which $\mathrm{d}\sigma$ denotes the area element of the toroidal surface. When there are $M$ point vortices located at $v_k$ with the strength $\Gamma_k$, $k = 1,\dots,n$ on the surface of the torus, the Gauss constraint (18) for the vorticity distribution (17) is equivalent to

$$\iint_{\mathbb{T}_\alpha} \mathrm{e}^{-2\psi}\,\mathrm{d}\sigma - \sum_{j=1}^{n} \Gamma_j = 0, \tag{19}$$

since the Gauss-Bonnet theorem and the definition of the $\delta$-measure assure that

$$\iint_{\mathbb{T}_\alpha} \kappa(\mathbb{T}_\alpha)\,\mathrm{d}\sigma = 2\pi\chi(\mathbb{T}_\alpha) = 0, \qquad \iint_{\mathbb{T}_\alpha} \delta_{v_j}\,\mathrm{d}\sigma = 1 \quad \text{for } j = 1,\dots,n,$$

where $\chi(\mathscr{M})$ is the Euler characteristic of the manifold $\mathscr{M}$. The first term in (19) is calculated as follows:

$$\begin{aligned}\iint_{\mathbb{T}_\alpha} \mathrm{e}^{-2\psi}\,\mathrm{d}\sigma &= 4\iint_{\mathbb{T}_\alpha} \frac{|\zeta|^2|f'(\zeta)|^2}{(1+|f(\zeta)|^2)^2(\alpha-\cos\theta)^2}\,\mathrm{d}\sigma \\ &= -2\mathrm{i}\iint_{D_\zeta} \frac{|f'(\zeta)|^2}{(1+|f(\zeta)|^2)^2}\,\mathrm{d}\zeta\wedge\mathrm{d}\overline{\zeta} \\ &= -2\mathrm{i}\iint_{D_\zeta} \frac{\partial}{\partial\overline{\zeta}}\left(\frac{f'(\zeta)\overline{f(\zeta)}}{1+|f(\zeta)|^2}\right)\mathrm{d}\zeta\wedge\mathrm{d}\overline{\zeta} \\ &= 2\mathrm{i}\oint_{\partial D_\zeta} \frac{f'(\zeta)\overline{f(\zeta)}}{1+|f(\zeta)|^2}\,\mathrm{d}\zeta. \end{aligned} \tag{20}$$

The Gauss constraint (19) now takes the form

$$2\mathrm{i}\oint_{\partial D_\zeta} \frac{f'(\zeta)\overline{f(\zeta)}}{1+|f(\zeta)|^2}\mathrm{d}\zeta - \sum_{j=1}^{n} \Gamma_j = 0, \tag{21}$$

and needs to be independently verified for every choice of the function $f(\zeta)$.

Finally, in order that the solution becomes a vortex crystal, it is sufficient and necessary that the configuration of point vortices is in an equilibrium state, which yields an additional constraint. Suppose that $\nu_0 \in D_\zeta$ is a zero of $f'(\zeta)$ with degree $m$. Then there is a point vortex at $\zeta = \nu_0$ with the strength $2\pi m$. The velocity field at this point is then calculated by subtracting the self-induced singular component (16) from the stream function Newton (2001); Saffman (1992); Sakajo and Shimizu (2016). That is to say, the evolution equation of the point vortex is given by

$$\frac{\mathrm{d}\overline{\nu}_0}{\mathrm{d}t} = 2\mathrm{i}\lambda^{-2}(\nu_0,\overline{\nu}_0)\frac{\partial}{\partial \nu_0}\widetilde{\psi}(\nu_0,\overline{\nu}_0), \tag{22}$$

in which the modified stream function $\widetilde{\psi}(\nu_0,\overline{\nu}_0)$ is defined by

$$\begin{aligned}\widetilde{\psi}(\nu_0,\overline{\nu}_0) &= \lim_{\zeta\to\nu_0}\left(\psi(\zeta,\overline{\zeta}) + m\log\widehat{d}(\zeta,\nu_0)\right) \\ &= \lim_{\zeta\to\nu_0}\left(\psi(\zeta,\overline{\zeta}) + m\log\left[\frac{(\alpha-\cos\theta_0)}{|\nu_0|}|\zeta-\nu_0|\right]\right).\end{aligned} \tag{23}$$

With the same calculation as (11), the point vortex at $\zeta = \nu_0$ stays at the same location, when we have

$$\nu_0\frac{\partial}{\partial \nu_0}\widetilde{\psi}(\nu_0,\overline{\nu}_0) = 0. \tag{24}$$

For a given doubly periodic function $f(\zeta)$ on $D_\zeta$, substituting it into the formula (15), we identify the locations of point vortices from the solution and confirm whether the Gauss condition (19) as well as the stationary condition (24).

## III. STEADY SOLUTIONS IN TERMS OF WEIERSTRASS $\wp$-FUNCTION

### A. A solution with four antipodal quantized point vortices

In this section we describe solutions to the modified Liouville equation (5) given in terms of the doubly-periodic Weierstrass $\wp$-function. A brief discussion of the $\wp$-function is provided in appendix A. We choose the analytic function $f(\zeta)$ in the stream function (15) as $f(\zeta) = \wp(-\mathrm{i}\log\zeta)$, which is defined on the annular domain $D_\zeta = \{\zeta \in \mathbb{C}\,|\,\rho < |\zeta| \leqq 1\}$ shown in figure

1. The domain $D_\zeta$ is related to the fundamental domain $D_z$ given by (A1) via the simple mapping $z = -\mathrm{i}\log\zeta$. The half-periods of $\wp(z)$ are $\omega_1 = \pi$ and $\omega_3 = -\frac{\mathrm{i}}{2}\log\rho$. The function $f(\zeta)$ is doubly periodic in $D_\zeta$, since

$$f(\zeta(\theta+2\pi,\phi)) = f(\rho\zeta) = \wp(-\mathrm{i}\log(\rho\zeta)) = \wp(-\mathrm{i}\log\zeta - \mathrm{i}\log\rho) = \wp(-\mathrm{i}\log\zeta) = f(\zeta),$$
$$f(\zeta(\theta,\phi+2\pi)) = f(\zeta),$$

by the definition of the stereographic projection (7). Substituting for $f(\zeta)$ and using $f'(\zeta) = -\frac{\mathrm{i}}{\zeta}\wp'(-\mathrm{i}\log\zeta)$ in (15), we obtain the stream function

$$\psi(\zeta,\overline{\zeta}) = -\frac{1}{2}\log\left[\frac{4|\wp'(-\mathrm{i}\log\zeta)|^2}{(1+|\wp(-\mathrm{i}\log\zeta)|^2)^2(\alpha-\cos\theta)^2}\right]. \tag{25}$$

Recall that $\wp(z)$ has a double pole at the origin $z = 0 \equiv \omega_0$, and $\wp'(z)$ has three simple zeros at the half-periods $\omega_1, \omega_3$ and at $\omega_2 = \omega_1 + \omega_3$. Hence, the stream function (25) has four logarithmic singularities, located at the points $v_k = \exp(\mathrm{i}\omega_k) \in D_\zeta$, $k = 0,1,2,3$, i.e., $v_0 = 1$, $v_1 = -1$, $v_2 = -\sqrt{\rho}$ and $v_3 = \sqrt{\rho}$. Each of these logarithmic singularities corresponds to a point vortex, and it can be verified using (A3) and (A4) that they all have the same strength $+2\pi$. There are thus four identical point vortices located at the antipodal positions of the toroidal surface $\mathbb{T}_\alpha$, namely $(\theta_0,\phi_0) = (0,0)$, $(\theta_1,\phi_1) = (0,\pi)$, $(\theta_2,\phi_2) = (\pi,\pi)$ and $(\theta_3,\phi_3) = (\pi,0)$.

The Gauss condition (21) is calculated as in Sakajo (2019a). The second term gives $\sum\Gamma_k = +8\pi$, and after substituting for $f(\zeta)$ the first term is

$$2\mathrm{i}\oint_{\partial D_\zeta}\frac{f'(\zeta)\overline{f(\zeta)}}{1+|f(\zeta)|^2}d\zeta = 2\mathrm{i}\oint_{\partial D_\zeta}\frac{\wp'(-\mathrm{i}\log\zeta)\overline{\wp(-\mathrm{i}\log\zeta)}}{1+|\wp(-\mathrm{i}\log\zeta)|^2}\left(-\frac{\mathrm{i}}{\zeta}\right)\mathrm{d}\zeta = 2\mathrm{i}\oint_{\partial D_z}\frac{\wp'(z)\overline{\wp(z)}}{1+|\wp(z)|^2}\mathrm{d}z. \tag{26}$$

Using (A3) and (A4) we find

$$\wp'(z)\overline{\wp(z)} = -\frac{2}{z|z|^4}(1+o(z^3))(1+o(\overline{z}^3)), \quad 1+|\wp(z)|^2 = \frac{1}{|z|^4}(1+o(|z|^3)),$$

so that we have

$$\frac{\wp'(z)\overline{\wp(z)}}{1+|\wp(z)|^2} = -\frac{2}{z}(1+o(|z|)), \quad |z|\to 0,$$

which means that the integrand of (26) has a simple pole at the origin with residue $-2$. Accordingly, owing to the doubly periodicity of the integrand, the integral (26) becomes

$$2\mathrm{i}\oint_{\partial D_z}\frac{\wp'(z)\overline{\wp(z)}}{1+|\wp(z)|^2}\mathrm{d}z = 2\mathrm{i}\cdot\lim_{\varepsilon\to 0}\oint_{|z|=\varepsilon}\frac{\wp'(z)\overline{\wp(z)}}{1+|\wp(z)|^2}\mathrm{d}z = 2\mathrm{i}\cdot 2\pi\mathrm{i}\cdot(-2) = 8\pi.$$

This shows that the Gauss condition (21) is satisfied.

We turn now to the stationary condition (24) for the point vortices at $\zeta = \nu_k$, $k = 0,1,2,3$. The modified stream function (23) is given by (using $m = 1$)

$$\begin{aligned}\widetilde{\psi}(\nu_k, \overline{\nu}_k) &= \lim_{\zeta\to\nu_k}\left(-\frac{1}{2}\log\left[\frac{4|\wp'(-\mathrm{i}\log\zeta)|^2}{(1+|\wp(-\mathrm{i}\log\zeta)|^2)^2(\alpha-\cos\theta)^2}\right]+\log\left[\frac{(\alpha-\cos\theta_k)}{|\nu_k|}|\zeta-\nu_k|\right]\right)\\ &= \lim_{\zeta\to\nu_k}\left(-\frac{1}{2}\log\left[\frac{4|\nu_k\wp'(-\mathrm{i}\log\zeta)|^2}{(1+|\wp(-\mathrm{i}\log\zeta)|^2)^2|\zeta-\nu_k|^2}\right]\right)+2\log(\alpha-\cos\theta_k).\end{aligned}$$

To proceed, we split into two cases, considering first the point vortices at $\zeta = \nu_k$, $k = 1,2,3$. Owing to $\wp'(\omega_k) = 0$ for $\omega_k = -\mathrm{i}\log\nu_k$, $k = 1,2,3$, we have the local behaviour

$$\wp'(-\mathrm{i}\log\zeta)-\wp'(-\mathrm{i}\log\nu_k) = -\frac{\mathrm{i}}{\nu_k}\wp''(-\mathrm{i}\log\nu_k)(\zeta-\nu_k)+o(\zeta-\nu_k), \qquad \zeta\to\nu_k,$$

from which we can calculate the limit

$$\lim_{\zeta\to\nu_k}\frac{|\nu_k\wp'(-\mathrm{i}\log\zeta)|^2}{(1+|\wp(-\mathrm{i}\log\zeta)|^2)^2|\zeta-\nu_k|^2} = \frac{|\wp''(-\mathrm{i}\log\nu_k)|^2}{(1+|\wp(-\mathrm{i}\log\nu_k)|^2)^2}.$$

After a little algebra, this gives us the modified stream function

$$\widetilde{\psi}(\nu_k,\overline{\nu}_k) = -\log 2-\frac{1}{2}\log|\wp''(-\mathrm{i}\log\nu_k)|^2+\log(1+|\wp(-\mathrm{i}\log\nu_k)|^2)+2\log(\alpha-\cos\theta_k).$$

The velocity field at $\zeta = \nu_k$ is then

$$\nu_k\frac{\partial}{\partial\nu_k}\widetilde{\psi}(\nu_k,\overline{\nu}_k) = \frac{\mathrm{i}}{2}\frac{\wp'''(-\mathrm{i}\log\nu_k)}{\wp''(-\mathrm{i}\log\nu_k)}-\mathrm{i}\frac{\wp'(-\mathrm{i}\log\nu_k)\overline{\wp(-\mathrm{i}\log\nu_k)}}{1+|\wp(-\mathrm{i}\log\nu_k)|^2}-\sin\theta_k = 0,$$

where we have used (A2) and the fact that $\theta_k = 0$ or $\pi$ for $k = 1,2,3$.

In the case $k = 0$ ($z = 0$, $\nu_0 = 1$, and $\theta_0 = 0$) it follows from (A3) and (A4) that

$$\frac{|\wp'(z)|^2}{(1+|\wp(z)|^2)^2} = \frac{\frac{4}{|z|^6}(1+o(|z|^3))}{\frac{1}{|z|^8}(1+o(|z|^3))} = 4|z|^2(1+o(|z|^3)), \qquad z\to 0.$$

Accordingly, we have

$$\log\left[\frac{|\wp'(-\mathrm{i}\log\zeta)|^2}{(1+|\wp(-\mathrm{i}\log\zeta)|^2)^2|\zeta-1|^2}\right] = \log\left[\left|\frac{2\log\zeta}{\zeta-1}\right|^2\left(1+o(|\zeta-1|^3)\right)\right]\to\log 4, \quad \zeta\to 1,$$

which yields

$$\nu_0\frac{\partial}{\partial\nu_0}\widetilde{\psi}(\nu_0,\overline{\nu}_0) = -\sin\theta_0 = 0.$$

Thus the four point vortices at the antipodal locations of the toroidal surface are stationary and the stream function (25) provides a steady solution of the incompressible Euler equation.

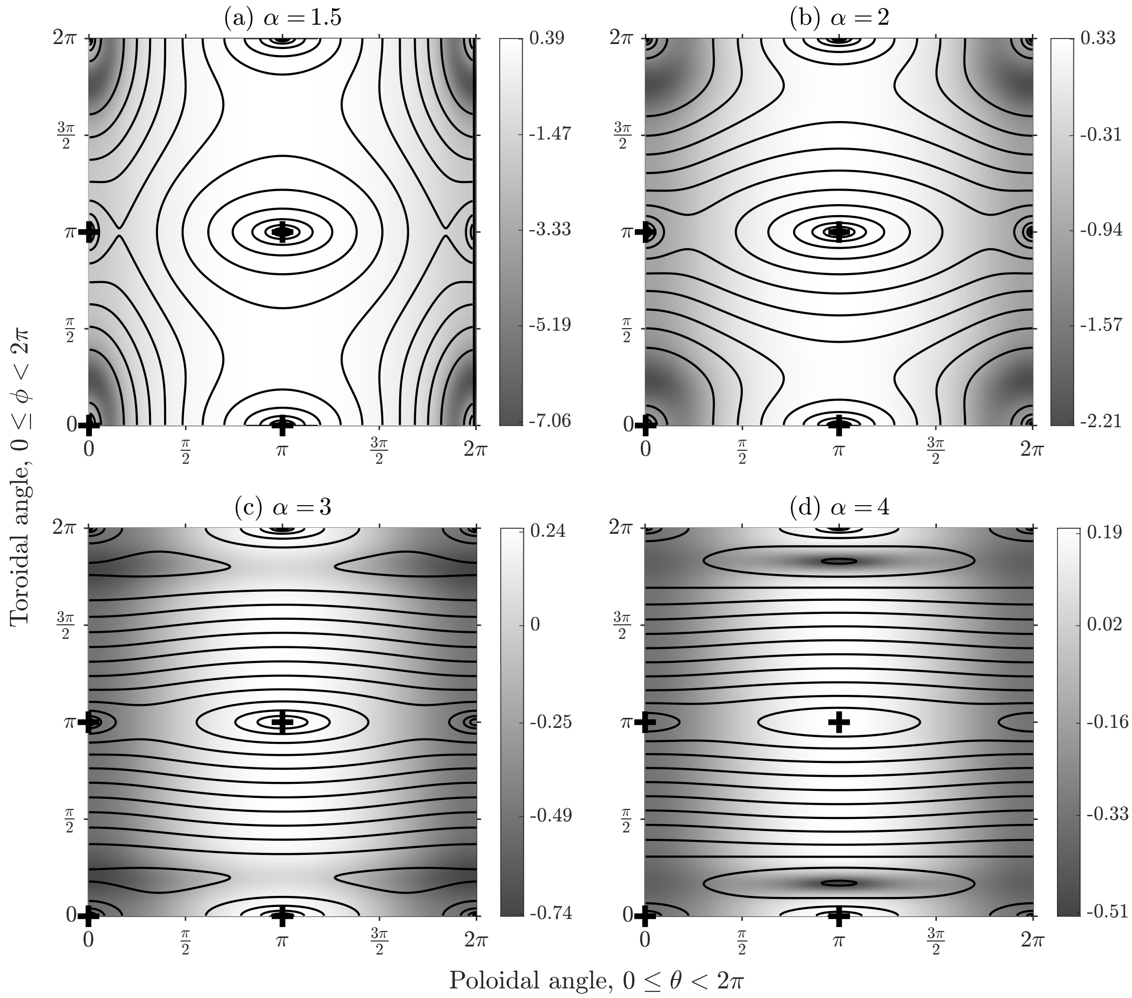


FIG. 2. Streamline contour plots, vorticity heatmaps, and embedded point vortices (+) corresponding to the stream function (25).

Figure 2 shows some example solutions for selected values of $\alpha$ and we see the topology of the flow change as $\alpha$ is varied. There are four point vortices with strength $2\pi$ embedded in the smooth background vorticity $\Omega_{\mathrm{sm}} = -\mathrm{e}^{-2\psi} + \kappa(\mathbb{T}_\alpha)$ at $(\theta,\phi) \in \{(0,0),(0,\pi),(\pi,0),(\pi,\pi)\}$. A ring of smooth vorticity around the point vortex at $(0,0)$ is seen in (a) and (b). As $\alpha$ increases, we see the predominant flow direction shift from along $\phi$ to along $\theta$. The background vorticity becomes smoother with increasing $\alpha$ in the sense that the difference between the minima and maxima of $\Omega_{\mathrm{sm}}$ decreases.

## B. $N$-ring configuration

We construct a steady solution with more quantized point vortices. Instead of using the stereographic projection (7), we introduce a map

$$\zeta = \zeta_N(\theta,\phi) = \exp(r_c(\theta))\mathrm{e}^{iN\phi}$$

for a fixed positive integer $N$. For each $k = 0,\ldots,N-1$, the map $\zeta_N$ defines a bijection from $T_k^N$ to $D_\zeta$, where

$$T_k^N = (\theta,\phi) \in (\mathbb{R}/2\pi\mathbb{Z}) \times \left[\frac{2\pi}{N}k, \frac{2\pi}{N}(k+1)\right)$$

for $k = 0,\ldots,N-1$. Since the toroidal surface is divided into $N$ domains with $T_k^N$, the map $z = -\mathrm{i}\log\zeta$ gives rise to a many-to-one map from $\mathbb{T}_\alpha$ to $D_z$. Hence, the pre-image of a point $D_z$ with respect to this map consists of $N$ points on $\mathbb{T}_\alpha$ that are equally spaced along the line of a latitude of the toroidal surface, i.e. an $N$-ring configuration.

The choice of the analytic function is then

$$f(\zeta) = f(\zeta_N(\theta,\phi)) = \wp(-\mathrm{i}\log\zeta_N(\theta,\phi)).$$

Since

$$f'(\zeta) = \left(\frac{1}{2\mathrm{i}\zeta}\frac{\partial}{\partial\phi} - \frac{\alpha-\cos\theta}{2\zeta}\frac{\partial}{\partial\theta}\right)\wp(-\mathrm{i}\log\zeta_N(\theta,\phi)) = -\frac{\mathrm{i}(N+1)}{2\zeta}\wp'(-\mathrm{i}\log\zeta_N(\theta,\phi)),$$

we obtain the following new analytic solution,

$$\psi(\zeta,\overline{\zeta}) = -\frac{1}{2}\log\left[\frac{(N+1)^2|\wp'(-\mathrm{i}\log\zeta_N(\theta,\phi))|}{(1+|\wp(-\mathrm{i}\log\zeta_N(\theta,\phi))|^2)^2(\alpha-\cos\theta)^2}\right]. \tag{27}$$

The analytic solution is apparently doubly periodic on $D_\zeta$ owing to the definition of $f(\zeta)$. Since there exist the three zeros of $\wp'(z)$ at $z = \omega_1,\omega_2,\omega_3$ and the double zero at $z = 0(=\omega_0)$ in $D_z$ and they are pulled back to $4N$ points on $\mathbb{T}_\alpha$, this solution contains a $4N$ quantized point vortices with the strength $2\pi$. The configuration of the $4N$ point vortices is two $2N$-rings where $2N$ point vortices are equally arranged along the line of latitudes $\theta = 0,\ \pi$, namely $(\theta_k,\phi_k) = (0,\frac{\pi k}{N})$ and $(\pi,\frac{\pi k}{N})$ for $k = 0,\ldots,2N-1$. The solution satisfies the Gauss constraint (18), since the integration of $\mathrm{e}^{-2\psi}$ over the toroidal surface is divided into $N$ identical integrations over $D_z$, for each of which the Gauss constraint is satisfied. It is also easy to show the $4N$ point vortices are in a fixed equilibrium state, since the calculation of (24) proceeds in the same way as in the antipodal case on $D_z$ and, additionally, their locations are $\theta_k = 0$ and $\pi$.

Let us finally note another choice of the function

$$f(\zeta)=\wp\left(-\mathrm{i}\log\zeta^N\right) \tag{28}$$

for a fixed positive integer $N$. Owing to $\zeta^N=\exp(Nr_c(\theta))\mathrm{e}^{iN\phi}$, it gives rise to a bijection from $T^N_{k_1,k_2}$ from $D_z$, in which

$$T^N_{k_1,k_2}=(\theta,\phi)\in\left[\frac{2\pi}{N}k_1,\frac{2\pi}{N}(k_1+1)\right)\times\left[\frac{2\pi}{N}k_2,\frac{2\pi}{N}(k_2+1)\right)$$

for $k_1,k_2=0,1,\ldots,N-1$. Since the toroidal surface is divided into the $N^2$ subdomains, the map $z=-i\log\zeta^N(\theta,\phi)$ becomes a many-to-one map from $\mathbb{T}_\alpha$ to $D_z$. Substitution of (28) into (15) yields an analytic solution formally. It is easy to see that the solution is doubly periodic and satisfies the Gauss constraint. The zeros of $\wp'(z)$ and the double pole of $\wp(z)$ in the fundamental domain $D_z$ are pulled back on the $4N^2$ point vortices with the strength $2\pi$ consisting of $2N$ $2N$-rings on the toroidal surface. However, this configuration is not a fixed equilibrium, since they do not satisfy the stationary condition.

## IV. STEADY SOLUTIONS IN TERMS OF LOXODROMIC FUNCTIONS

In this section we consider solutions to the modified Liouville equation (5) given in terms of loxodromic functions. The special functions used here are the Schottky-Klein prime function (Crowdy, 2020) and its derivatives defined on the annulus $D_\zeta=\{\zeta\in\mathbb{C}\,|\,\rho<|\zeta|\leqq 1\}$ shown in figure 1. We call any function $G(\zeta)$ defined on $D_\zeta$ a loxodromic function if it is invariant under $\zeta\mapsto\rho\zeta$, i.e. $G(\zeta)=G(\rho\zeta)$. Basic properties of the prime function and its derivatives are reviewed in appendix B and will be referred to throughout this section. We consider the function

$$f(\zeta)=W_0(\zeta)\equiv\sum_{k=1}^{\widehat{n}}\Big(K(\zeta/a_k,\sqrt{\rho})-K(\zeta/b_k,\sqrt{\rho})\Big),\qquad \widehat{n}\in\mathbb{N}, \tag{29}$$

on $D_\zeta$, where $a_k,b_k\in D_\zeta$ with $a_k\neq b_k$, $k=1,\ldots,\widehat{n}$, are parameters. Here, the $K$-function is defined by (B2). It can be proven using (B3) that $W_0(\zeta)$ is a loxodromic function satisfying $W_0(\rho\zeta)=W_0(\zeta)$. Note that it follows from (B4) that $W_0(\zeta)$ has $2\widehat{n}$ simple poles, located at $\zeta=a_k,b_k$ for $k=1,\ldots,\widehat{n}$.

We now introduce a second function

$$W_1(\zeta)\equiv\zeta f'(\zeta)=\sum_{k=1}^{\widehat{n}}\Big(L(\zeta/a_k,\sqrt{\rho})-L(\zeta/b_k,\sqrt{\rho})\Big), \tag{30}$$

where the $L$-function is defined by (B5). We see using (B10) that $W_1(\zeta)$ is also a loxodromic function, and from (B9) we see that it has $2\widehat{n}$ double poles, one each at $\zeta = a_k$ and $\zeta = b_k$, for $k = 1,\dots,\widehat{n}$. It thus has $4\widehat{n}$ zeros, located at say $\zeta = \nu_j$, $j = 1,\dots,4\widehat{n}$, with multiplicity in the annulus $D_\zeta$ according to the general theory of elliptic functions Hurwitz and Courant (1944). We can now rewrite the stream function (15) as

$$\psi(\zeta,\overline{\zeta}) = -\frac{1}{2}\log\left[\frac{4|W_1(\zeta)|^2}{(1+|W_0(\zeta)|^2)^2(\alpha-\cos\theta)^2}\right] \tag{31}$$

The function $W_0(\zeta)$ consists of $\widehat{n}$ simple poles at $a_k$ and $\widehat{n}$ simple poles at $b_k$. Following the discussion in §II, we see that the stream function (31) is regular at the $2\widehat{n}$ simple poles $\zeta = a_k, b_k$, $k = 1,\dots,\widehat{n}$. However, the stream function has $4\widehat{n}$ point vortices (logarithmic singularities) at the zeros $\nu_j$ of $W_1(\zeta)$. If these point vortices are stationary, and if further the Gauss constraint (21) is satisfied, then (31) provides a steady solution of the modified Liouville equation (5).

Let us next confirm whether the stream function (31) satisfies the Gauss condition (21). Since the exact solution contains $n = 4\widehat{n}$ point vortices with the identical strength $\Gamma_j = 2\pi$, the total circulation owing to the point vortices is given by $\sum_{j=1}^{n}\Gamma_j = 8\pi\widehat{n}$. In the meantime, we need to evaluate the integral in the Gauss constraint (21) with $f(\zeta)$ given by (29). To do this, note that the only singularities of the quantity $W_0'(\zeta)\overline{W_0(\zeta)}/(1+|W_0(\zeta)|^2)$ are at the poles of $W_0(\zeta)$, so we investigate its behavior in the neighborhood of $\zeta = a_k$ and $\zeta = b_k$. We find from (29) and (B4) that near these singularities

$$\frac{W_0'(\zeta)\overline{W_0(\zeta)}}{1+|W_0(\zeta)|^2} \sim \frac{W_0'(\zeta)}{W_0(\zeta)} = \frac{\mathrm{d}}{\mathrm{d}\zeta}\log W_0(\zeta) = \begin{cases} -\dfrac{1}{\zeta-a_k} + O(1) & \text{as } \zeta \to a_k, \\[2ex] -\dfrac{1}{\zeta-b_k} + O(1) & \text{as } \zeta \to b_k, \end{cases}$$

for $k = 1,\dots,\widehat{n}$. This indicates that this function has a simple pole with residue $-1$ at each $\zeta = a_k, b_k$, $k = 1,\dots,\widehat{n}$. Notice that the residues at $\zeta = a_k$ and $\zeta = b_k$ are both equal. Accordingly, the first term in (21) gives,

$$\begin{aligned} 2\mathrm{i}\oint_{\partial D_\zeta}\frac{W_0'(\zeta)\overline{W_0(\zeta)}}{1+|W_0(\zeta)|^2}\mathrm{d}\zeta &= 2\mathrm{i}\cdot\lim_{\varepsilon\to 0}\sum_{k=1}^{\widehat{n}}\left[\oint_{|\zeta-a_k|=\varepsilon}\frac{W_0'(\zeta)\overline{W_0(\zeta)}}{1+|W_0(\zeta)|^2}\mathrm{d}\zeta + \oint_{|\zeta-b_k|=\varepsilon}\frac{W_0'(\zeta)\overline{W_0(\zeta)}}{1+|W_0(\zeta)|^2}\mathrm{d}\zeta\right] \\ &= 2\mathrm{i}\cdot 2\pi\mathrm{i}\cdot\sum_{k=1}^{\widehat{n}}[(-1)+(-1)] \\ &= 8\pi\widehat{n}, \end{aligned}$$

showing that the Gauss condition (21) is satisfied by the stream function (31).

Finally, we derive the stationary condition (24) for the point vortex at $\zeta = \nu_j,\ j = 1, \ldots, 4\widehat{n}$. Since this point vortex (of strength $2\pi$) appears as a simple zero of $W_1(\zeta)$, we have $m = 1$ in (23). By definition, let us first compute from (31):

$$\psi(\zeta, \overline{\zeta}) + \log\left[\frac{\alpha - \cos\theta}{|\nu_j|}|\zeta - \nu_j|\right] = -\frac{1}{2}\log\left|\frac{\nu_j(W_1(\zeta) - W_1(\nu_j))}{\zeta - \nu_j}\right|^2 + \log\left(1 + |W_0(\zeta)|^2\right)$$
$$+\log(\alpha - \cos\theta) + \log(\alpha - \cos\theta_j) - \log 2,$$

where we have used the fact that $W_1(\nu_j) = 0$. The modified stream function is then obtained by taking the limit $\zeta \to \nu_j$:

$$\widetilde{\psi}(\nu_j, \overline{\nu}_j) = -\frac{1}{2}\log|W_2(\nu_j)|^2 + \log(1 + |W_0(\nu_j)|^2) + 2\log(\alpha - \cos\theta_j) - \log 2. \tag{32}$$

Here we have defined the new function

$$W_2(\zeta) \equiv \zeta W_1'(\zeta) = \sum_{k=1}^{\widehat{n}} \Big(M(\zeta/a_k, \sqrt{\rho}) - M(\zeta/b_k, \sqrt{\rho})\Big), \tag{33}$$

in terms of the $M$-function in (B6). Applying $\nu_j \frac{\partial}{\partial \nu_j}$ to the modified stream function (32) we get

$$\nu_j \frac{\partial \widetilde{\psi}}{\partial \nu_j} = -\frac{1}{2}\frac{W_3(\nu_j)}{W_2(\nu_j)} + \frac{W_0'(\nu_j)\overline{W_0(\nu_j)}}{1 + |W_0(\nu_j)|^2} - \sin\theta_j = -\frac{1}{2}\frac{W_3(\nu_j)}{W_2(\nu_j)} - \sin\theta_j,$$

where we have defined the new functions

$$W_3(\zeta) \equiv \zeta W_2'(\zeta) = \sum_{k=1}^{\widehat{n}} \Big(N(\zeta/a_k, \sqrt{\rho}) - N(\zeta/b_k, \sqrt{\rho})\Big), \tag{34}$$

in terms of the $N$-function in (B7). We have also used $W_1(\nu_j) = \nu_j W_0'(\nu_j) = 0$, and calculated using (12) that

$$2\nu_j \frac{\partial}{\partial \nu_j}\log(\alpha - \cos\theta_j) = -\sin\theta_j.$$

In summary, the stationary condition (24) is reduced to

$$\frac{W_3(\nu_j)}{W_2(\nu_j)} + 2\sin\theta_j = 0 \quad \text{for } j = 1, \ldots, 4\widehat{n}. \tag{35}$$

In (35) the angle $\theta_j$ is related to $\nu_j$ via $\log|\nu_j| = r_c(\theta_j)$, where $r_c(\theta_j)$ is given by (8). The stationary condition can be further simplified by considering symmetric solutions, which have $\theta_j = 0$ or $\pi$ so that $\sin\theta_j = 0$ for all $j$. This provides a restriction on the location of the zeros $\nu_j$,

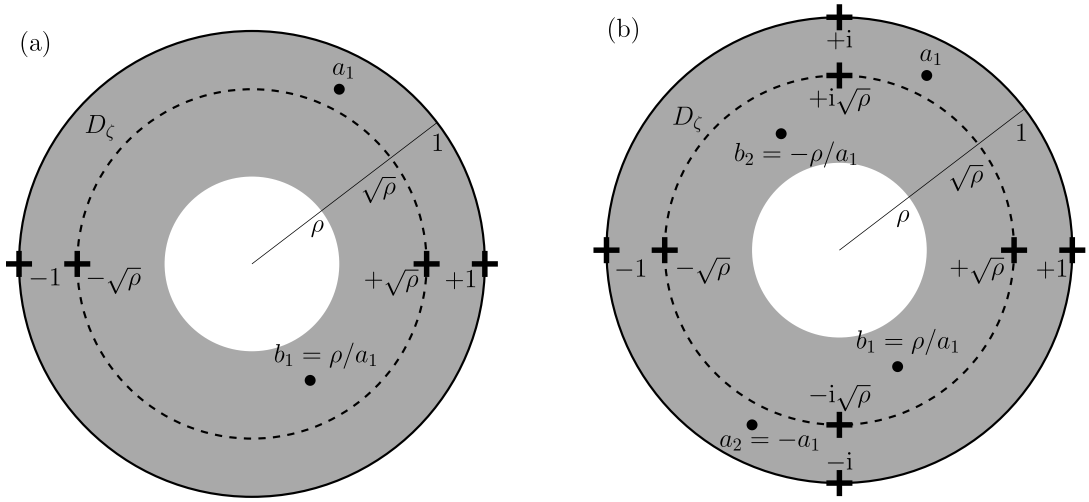


FIG. 3. Schematic showing the location of poles $a_k, b_k$ (•) and point vortices (+), in the annulus $D_\zeta$, for the stream function (31). (a) We have taken $\hat{n} = 1$ and set $b_1 = \rho/a_1$. The stream function is then a function of the arbitrary parameter $a_1$, with the four point vortices in the solution fixed at $\pm 1, \pm\sqrt{\rho}$. (b) We have taken $\hat{n} = 2$ and set $b_1 = \rho/a_1$, $a_2 = -a_1$, and $b_2 = -\rho/a_1$. The stream function is again a function of $a_1$ with eight point vortices fixed at $\pm 1, \pm\sqrt{\rho}, \pm\mathrm{i}, \pm\mathrm{i}\sqrt{\rho}$. See §IV A for details. Some examples of vorticity and streamline plots for different choices of $a_1$ are shown in figures 4 and 5 for $\hat{n} = 1$ and in figure 6 for $\hat{n} = 2$.

since from (8) we get $\log|\nu_j| = r_c(0) = 0$ or $\log|\nu_j| = r_c(\pi) = -\pi\mathscr{A} = \log\sqrt{\rho}$. Thus for such symmetric solutions we must have $|\nu_j| = 1$ or $|\nu_j| = \sqrt{\rho}$ leading to the stationary point vortex condition in the form

$$W_3(\nu_j) = 0, \quad |\nu_j| = 1 \text{ or } \sqrt{\rho}, \quad \text{for } j = 1, \ldots, 4\widehat{n}. \tag{36}$$

We note that $W_2(\nu_j) \neq 0$ for all $j$. The $M$ and $N$-functions, and hence $W_2$ and $W_3$, are all loxodromic functions. The properties (B10) and (B12) satisfied by the $L$ and $N$-functions are identical, while the corresponding property in (B11) differs by a sign. The condition (36) means that the four point vortices of the stationary solution are necessarily on the innermost and the outermost antipodal locations of the toroidal surface. We construct symmetric families of solutions to the modified Liouville equation, continuously dependent on a parameter, which satisfy (36), using these properties for any $\widehat{n}$.

## A. Examples with four point vortices

We consider the case when $\widehat{n} = 1$, in which $W_1(\zeta)$ has double poles at $a_1, b_1 \in D_\zeta$, $a_1 \neq b_1$, and four zeros. We now solve $W_1(\zeta) = 0$ to obtain the locations $v_1, v_2, v_3, v_4$ of point vortices contained in the exact solution (31). It is easy to verify that $\pm\sqrt{a_1 b_1}$ and $\pm\sqrt{a_1 b_1/\rho}$ are four zeros of $W_1(\zeta)$. Indeed using the properties (B10), we have

$$\begin{aligned} W_1(\pm\sqrt{a_1 b_1}) &= L(\pm\sqrt{a_1 b_1}/a_1, \sqrt{\rho}) - L(\pm\sqrt{a_1 b_1}/b_1, \sqrt{\rho}) \\ &= L(\pm\sqrt{b_1/a_1}, \sqrt{\rho}) - L(\pm\sqrt{a_1/b_1}, \sqrt{\rho}) \\ &= 0. \end{aligned}$$

We can similarly show that $W_1(\pm\sqrt{a_1 b_1/\rho}) = 0$:

$$\begin{aligned} W_1(\pm\sqrt{a_1 b_1/\rho}) &= L(\pm\sqrt{a_1 b_1/\rho}/a_1, \sqrt{\rho}) - L(\pm\sqrt{a_1 b_1/\rho}/b_1, \sqrt{\rho}) \\ &= L(\pm\sqrt{b_1/\rho a_1}, \sqrt{\rho}) - L(\pm\sqrt{a_1/\rho b_1}, \sqrt{\rho}) \\ &= L(\pm\sqrt{\rho a_1/b_1}, \sqrt{\rho}) - L(\pm\rho\sqrt{a_1/\rho b_1}, \sqrt{\rho}) \\ &= 0, \end{aligned}$$

where we have used (B10). Since $W_1(\zeta)$ is loxodromic, it follows that any $\rho$-multiple of these zeros are further zeros of $W_1(\zeta)$, for example $W_1(\pm\sqrt{\rho a_1 b_1}) = 0$. Depending on the values of $a_1$ and $b_1$ we can locate the four zeros of $W_1(\zeta)$ in $D_\zeta$.

The $N$-function satisfies the same properties as the $L$-function (see (B12)), and since we have used only these properties to find the zeros of $W_1(\zeta)$, we see that the function $W_3(\zeta)$ must also vanish at the zeros of $W_1(\zeta)$. The point vortex stationary condition (36) is thus automatically satisfied if we choose $v_j$ to be these zeros with $|v_j| = 1$ or $\sqrt{\rho}$. This last requirement is met if we choose $a_1$ and $b_1$ such that $|a_1 b_1| = \rho$, so that the positions of the point vortices are $v_1 = 1$, $v_2 = -1$, $v_3 = \sqrt{\rho}$, and $v_4 = -\sqrt{\rho}$ (see figure 3(a)). We thus have a family of solutions parametrised by $a_1$ (if we choose $b_1 = \rho/a_1$) in which the four stationary point vortices are fixed at $\pm 1, \pm\sqrt{\rho}$ as $|a_1|$ varies in the range $\sqrt{\rho} < |a_1| < 1$. We can restrict $|a_1|$ to be in this range without loss of generality because of the symmetry between $a_1$ and $b_1$; we disallow the value $a_1 = 1$ since then $b_1 = \rho$ and so $W_1(\zeta)$ is identically zero. Although setting $|a_1 b_1| = 1$ would also satisfy (36), this does not lead to a parametrised family of solutions since we need $a_1, b_1 \in D_\zeta$. However we obtain solutions when $|a_1| = |b_1| = 1$, for example $a_1 = \mathrm{i}$, $b_1 = -\mathrm{i}$ leads to four point vortices at $\pm 1, \pm\sqrt{\rho}$.

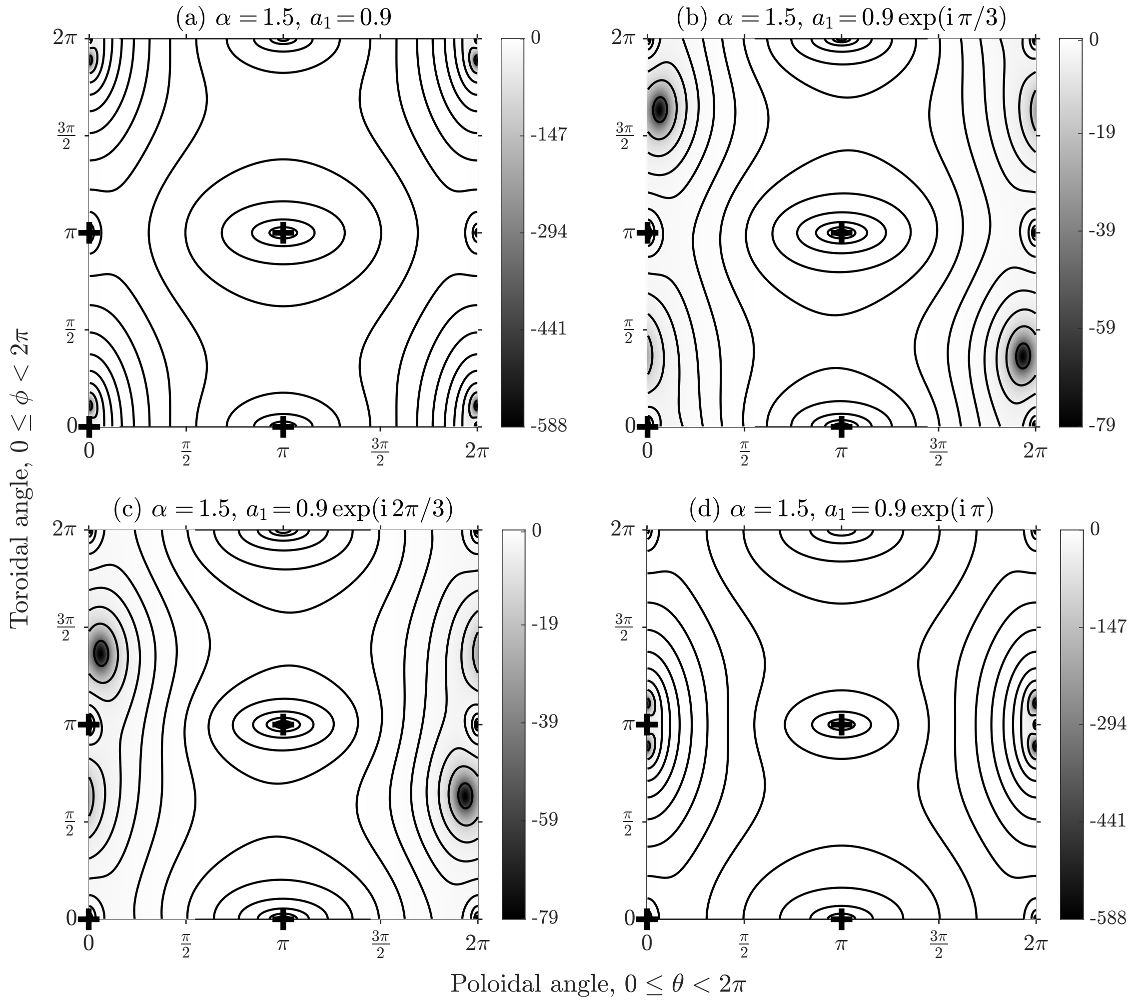


FIG. 4. Streamline contour plots, vorticity heatmaps, and embedded point vortices (+) in the $\theta$-$\phi$ plane corresponding to the stream function (31) for $\hat{n} = 1$ and $\alpha = 1.5$.

Figure 4 shows chosen example solutions for $\widehat{n} = 1$, corresponding to the schematic shown in figure 3(a). There are four point vortices embedded in the smooth background vorticity $\Omega_{\mathrm{sm}} = -\mathrm{e}^{-2\psi} + \kappa(\mathbb{T}_\alpha)$. These point vortices remain fixed at $(\theta, \phi) \in \{(0,0), (0,\pi), (\pi,0), (\pi,\pi)\}$ when $a_1$ is changed, as shown in the panels (a)–(d). However, the centers of the smooth vorticity move around and the values of the vorticity minima change as $a_1$ is varied. The solution behaves similarly in the parameter range $\pi < \arg(a_1) < 2\pi$. Figure 5 shows the same plots for $\alpha = 3$, in which we observe the changing of the flow topology, the motion of the smooth vorticity centers and the values of the vorticity minima (compare figures 4 and 5).

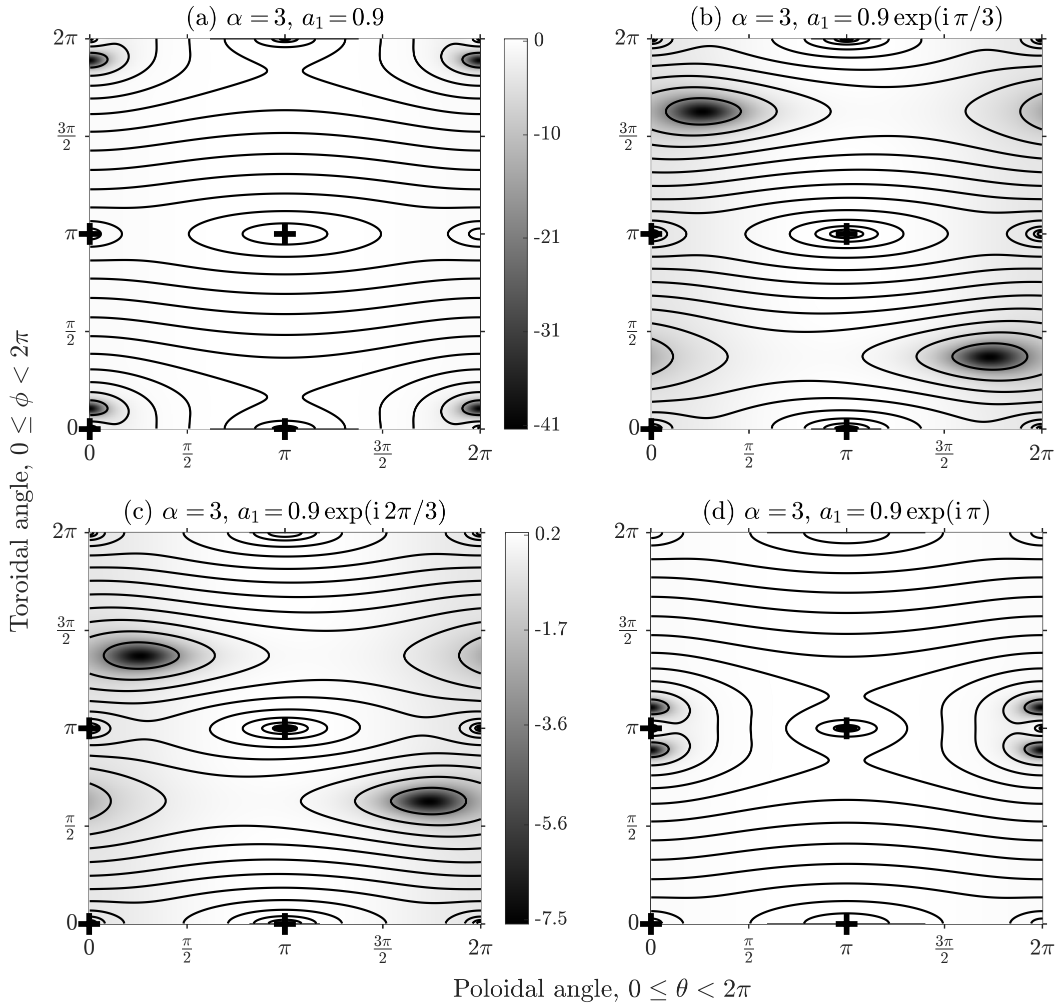


FIG. 5. Streamline contour plots, vorticity heatmaps, and embedded point vortices (+) in the $\theta$-$\phi$ plane corresponding to the stream function (31) for $\hat{n} = 1$ and $\alpha = 3$.

## B. Example with eight point vortices

We can generalise the preceding arguments for any $\widehat{n}$. Let us assume that $a_k$ and $b_k$, $k = 1, \ldots, \widehat{n}$, satisfy the following condition.

$$a_k b_k = \rho, \qquad a_k = a_1 \mathrm{e}^{\mathrm{i}(k-1)2\pi/\widehat{n}}, \qquad k = 1, \ldots, \widehat{n}. \tag{37}$$

Then, it is straightforward to show that

$$v_j = \begin{cases} \mathrm{e}^{\mathrm{i}(j-1)\pi/\widehat{n}} & \text{for} \quad j = 1, \ldots, 2\widehat{n}, \\ \sqrt{\rho}\,\mathrm{e}^{\mathrm{i}(j-1)\pi/\widehat{n}} & \text{for} \quad j = 2\widehat{n}+1, \ldots, 4\widehat{n}, \end{cases} \tag{38}$$

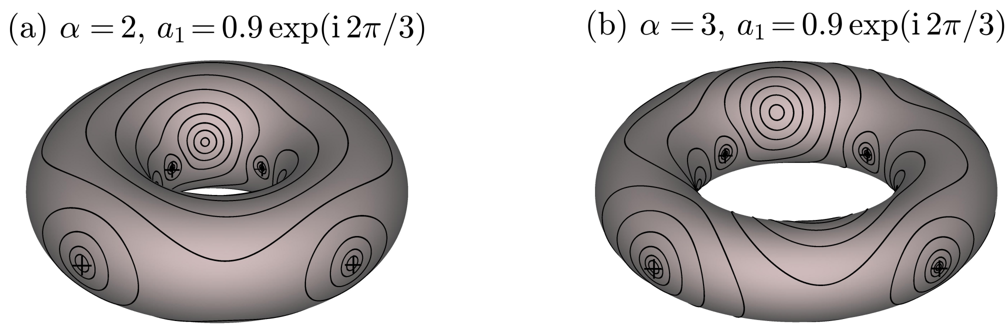


FIG. 6. Streamline contours projected on the torus, along with embedded point vortices (+), in the case $\hat{n}=2$ (vorticity heatmaps are not shown here).

are the zeros of $W_1(\zeta)$. Namely, we have using (B10) that

$$W_1(\nu_j) = \sum_{k=1}^{\widehat{n}} L(1/a_1 \mathrm{e}^{\mathrm{i}(-j+2k-1)\pi/\widehat{n}}, \sqrt{\rho}) - L(a_1 \mathrm{e}^{\mathrm{i}(j+2k-3)\pi/\widehat{n}}, \sqrt{\rho}) = 0,$$

for $j=1,\ldots,2\widehat{n}$, since $-j+2k-1$ and $j+2k-3$ run from 0 to $\widehat{n}-1$ for fixed $j$ and $k=1,\ldots,\widehat{n}$ with the periodicity $\mathrm{e}^{\mathrm{i}(\widehat{n})2\pi/\widehat{n}}=1$. We also have, using (B10), that

$$W_1(\nu_j) = \sum_{k=1}^{\widehat{n}} L(\sqrt{\rho}/a_1 \mathrm{e}^{\mathrm{i}(-j+2k-1)\pi/\widehat{n}}, \sqrt{\rho}) - L(\sqrt{\rho} a_1 \mathrm{e}^{\mathrm{i}(j+2k-3)\pi/\widehat{n}}, \sqrt{\rho}) = 0,$$

for $j=2\widehat{n}+1,\ldots,4\widehat{n}$. Since the function $N(\zeta)$ satisfies the same properties as $L(\zeta)$, we have $W_3(\nu_j)=0$ for $j=1,\ldots,4\widehat{n}$. Moreover, these zeros correspond to point vortices at the innermost and outermost locations of the torus, i.e., $\theta_j=0$ or $\pi$ (in other words $|\nu_j|=1$ or $\sqrt{\rho}$) for any $j$. Hence, the stationary condition (36) is satisfied.

The situation in the annulus for $\hat{n}=2$ and solutions parametrised by $a_1$ is shown as a schematic in figure 3(b). The streamline contours are projected onto the torus in figure 6 for (a) $\alpha=2$ and (b) $\alpha=3$. We choose $a_1=0.9\,\mathrm{e}^{\mathrm{i}2\pi/3}$, $b_1=\rho/a_1$, $a_2=-a_1$ and $b_2=\rho/a_1$. Four of the eight point vortices and one of the four smooth centers are visible from the viewing angle in figure 6.

## V. LIMIT SOLUTIONS

We can construct classes of "limit solutions" to the Liouville-type equation (5) by substituting $f(\zeta)=A(h(\zeta)+C)$, where $A\in\mathbb{R}$, $A>0$ and $C\in\mathbb{C}$ are constants, into the stream function (15):

$$\begin{aligned}\psi(\zeta,\overline{\zeta}) &= -\frac{1}{2}\log\left[\frac{A|h'(\zeta)|}{1+A^2|h(\zeta)+C|^2}\right]^2 - \frac{1}{2}\log\left[\frac{4|\zeta|^2}{(\alpha-\cos\theta)^2}\right] \\ &= +\log\left[\frac{1}{A|h'(\zeta)|} + A\frac{|h(\zeta)+C|^2}{|h'(\zeta)|}\right] - \frac{1}{2}\log\left[\frac{4|\zeta|^2}{(\alpha-\cos\theta)^2}\right].\end{aligned}$$

Note that since only $|A|$ would appear in the stream function above, we can take $A$ to be real and non-negative without any loss of generality. By adding and subtracting the constant term $\log A$ and taking the limits $A \to 0$ and $A \to \infty$, we obtain the following two *limit* solutions:

$$\psi_0(\zeta,\overline{\zeta}) = \lim_{A\to 0}\left[\psi(\zeta,\overline{\zeta}) + \log A\right] = -\log|h'(\zeta)| - \frac{1}{2}\log\left[\frac{4|\zeta|^2}{(\alpha-\cos\theta)^2}\right], \tag{39}$$

$$\psi_\infty(\zeta,\overline{\zeta}) = \lim_{A\to\infty}\left[\psi(\zeta,\overline{\zeta}) - \log A\right] = -\log\left[\frac{|h'(\zeta)|}{|h(\zeta)+C|^2}\right] - \frac{1}{2}\log\left[\frac{4|\zeta|^2}{(\alpha-\cos\theta)^2}\right]. \tag{40}$$

When we act the Laplace-Beltrami operator $\nabla^2_{\mathbb{T}_\alpha}$ on these limit solutions, the first terms vanish and the second terms become $-\kappa(\mathbb{T}_\alpha)$. Moreover, they contain pole vortices with the strength quantized by $2m\pi$, $m \in \mathbb{Z}$, at poles and zeros of the functions $h'(\zeta)$ and $h(\zeta)+C$ of degree $m$. Hence, they are solutions of

$$\nabla^2_{\mathbb{T}_\alpha}\psi = -\kappa(\mathbb{T}_\alpha) - \sum_{j=1}^{n}\Gamma_j\delta_{v_j}, \tag{41}$$

where $n$ point vortices with the strength $\Gamma_j$ exist at $v_j$ for $j = 1,\ldots,n$. The vorticity distribution on the toroidal surface is thus given by

$$-\Omega = -\kappa(\mathbb{T}_\alpha) - \sum_{j=1}^{n}\Gamma_j\delta_{v_j}. \tag{42}$$

It indicates that the limit solutions represent flows of $n$ point vortices embedded in the background vorticity distribution $\kappa(\mathbb{T}_\alpha)$. The Gauss condition is reduced to

$$\iint_{\mathbb{T}_\alpha}\Omega\,\mathrm{d}\sigma = \sum_{j=1}^{n}\Gamma_j = 0, \tag{43}$$

in which the contribution from the nonlinear term $\mathrm{e}^{-2\psi}$ is not included.

In what follows, as in Section 3, we consider two functions, i.e., the Weierstrass $\wp$ function $h(\zeta) = \wp(-i\log\zeta)$ and a loxodromic function $h(\zeta) = K(\zeta/a) - K(\zeta/b)$ for $a,b \in D_\zeta$ as examples of limit solutions.

## A. Weierstrass $\wp$-function

Choosing $h(\zeta) = \wp(-\mathrm{i}\log\zeta)$, the limit solution $\psi_0(\zeta,\overline{\zeta})$ given by (39) becomes

$$\psi_0(\zeta,\overline{\zeta}) = -\frac{1}{2}\log\left[\frac{4|\wp'(-\mathrm{i}\log\zeta)|^2}{(\alpha-\cos\theta)^2}\right]. \tag{44}$$

The derivative of the Weierstrass $\wp$-function, $\wp'(z)$, has three simple zeros at $z = \omega_1$, $\omega_2$, $\omega_3$, and a pole of degree three at $\omega_0 = 0$ (see §III). The stream function (44) thus contains three point vortices with strength $\Gamma_k = +2\pi$ each, at $v_k = \exp(\mathrm{i}\omega_k)$ for $k = 1,2,3$, and a point vortex with strength $\Gamma_0 = -6\pi$ at $v_0 = \exp(\mathrm{i}\omega_0) = 1$. Then the total point vortex circulation vanishes, namely $\Gamma_0+\Gamma_1+\Gamma_2+\Gamma_3 = 0$. Hence, the Gauss condition (43) is satisfied.

The stationary condition on the point vortices is checked for $\zeta = v_k$, $k = 1,2,3$ and $\zeta = v_0$ separately, since the strengths of the point vortices are different. For the point vortices with strengths $\Gamma_k = +2\pi$ at $\zeta = v_k$, $k = 1,2,3$, we get from (23) (where $m = 1$)

$$\begin{aligned}\widetilde{\psi}_0(v_k,\overline{v}_k) &= \lim_{\zeta\to v_k}\left(-\frac{1}{2}\log\left[\frac{4|\wp'(-\mathrm{i}\log\zeta)|^2}{(\alpha-\cos\theta)^2}\right]+\log\left[\frac{(\alpha-\cos\theta_k)}{|v_k|}|\zeta-v_k|\right]\right)\\ &= -\log 2+2\log(\alpha-\cos\theta_k)-\frac{1}{2}\log|v_k|^2-\frac{1}{2}\lim_{\zeta\to v_k}\log\left|\frac{\wp'(-\mathrm{i}\log\zeta)-\wp'(-\mathrm{i}\log v_k)}{\zeta-v_k}\right|^2\\ &= -\log 2+2\log(\alpha-\cos\theta_k)-\frac{1}{2}\log|\wp''(-\mathrm{i}\log v_k)|^2.\end{aligned}$$

Hence, it follows from (12) that

$$v_k\frac{\partial}{\partial v_k}\widetilde{\psi}_0(v_k,\overline{v}_k) = -\sin\theta_k+\frac{\mathrm{i}}{2}\frac{\wp'''(-\mathrm{i}\log v_k)}{\wp''(-\mathrm{i}\log v_k)} = 0, \qquad k = 1,2,3,$$

owing to (A2) and $\theta_1 = \theta_2 = \pi$, $\theta_3 = 0$. For the point vortex at $\zeta = v_0 = 1$ with strength $\Gamma_0 = -6\pi$, we get using (23) (with $m = -3$),

$$\begin{aligned}\widetilde{\psi}_0(v_0,\overline{v}_0) &= \lim_{\zeta\to v_0}\left(-\frac{1}{2}\log\left[\frac{4|\wp'(-\mathrm{i}\log\zeta)|^2}{(\alpha-\cos\theta)^2}\right]-3\log\left[\frac{(\alpha-\cos\theta_0)}{|v_0|}|\zeta-v_0|\right]\right)\\ &= -\log 2-2\log(\alpha-\cos\theta_0)+3\log|v_0|-\lim_{\zeta\to v_0}\log|(\zeta-v_0)^3\wp'(-\mathrm{i}\log\zeta)|\\ &= -2\log 2-2\log(\alpha-\cos\theta_0).\end{aligned}$$

Here, we have used (A4) to calculate

$$\lim_{\zeta\to v_0}\log|(\zeta-v_0)^3\wp'(-\mathrm{i}\log\zeta)| = \lim_{\zeta\to v_0}\log\left|-\frac{2v_0^3(\zeta/v_0-1)^3}{(-\mathrm{i}\log(\zeta/v_0))^3}(1+o(-\mathrm{i}\log\zeta)^3)\right| = \log|2v_0^3|.$$

Hence, we obtain

$$v_0\frac{\partial}{\partial v_0}\widetilde{\psi}_0(v_0,\overline{v}_0) = \sin\theta_0 = 0.$$

Consequently, the stream function $\psi_0(v_0,\overline{v}_0)$ gives rise to a stationary solution of the Euler equation. It is important to notice that it contains the quantized point vortices with the different strengths at the innermost and the outermost locations.

The other limit solution $\psi_\infty(\zeta,\overline{\zeta})$ is given by

$$\psi_\infty(\zeta,\overline{\zeta}) = -\frac{1}{2}\log\left[\frac{4}{(\alpha-\cos\theta)^2}\frac{|\wp'(-\mathrm{i}\log\zeta)|^2}{|\wp(-\mathrm{i}\log\zeta)+C|^4}\right]. \tag{45}$$

Since $\wp(z)$ has a double pole at $z=\omega_0=0$, the equation $\wp(z)+C=0$ has two zeros, say at $z=\widehat{\omega}_1$ and $\widehat{\omega}_2$. Hence, the solution contains four point vortices at $\nu_k=\exp(\mathrm{i}\omega_k)$ with strengths $\Gamma_k=+2\pi$ for $k=0,1,2,3$. There are two additional point vortices at $\widehat{\nu}_k=\exp(\mathrm{i}\widehat{\omega}_k)$ with strengths $\widehat{\Gamma}_k=-4\pi$ for $k=1,2$. Hence, the total circulation satisfies $\sum_{k=1}^{4}\Gamma_k+\sum_{k=1}^{2}\widehat{\Gamma}_k=0$. Hence, the Gauss condition (19) holds true.

We confirm if the stationary condition is satisfied by these six point vortices. First, consider the point vortices with strength $\Gamma_k=+2\pi$ at $\zeta=\nu_k=\exp(\mathrm{i}\omega_k)$, $k=1,2,3$. These point vortices are located at the zeros of $\wp'(-\mathrm{i}\log\zeta)$ and the modified stream function (23) in this case is (with $m=1$)

$$\begin{aligned}
\widetilde{\psi}_\infty(\nu_k,\overline{\nu}_k) &= \lim_{\zeta\to\nu_k}\left(-\frac{1}{2}\log\left[\frac{4}{(\alpha-\cos\theta)^2}\frac{|\wp'(-\mathrm{i}\log\zeta)|^2}{|\wp(-\mathrm{i}\log\zeta)+C|^4}\right]+\log\left[\frac{(\alpha-\cos\theta_k)}{|\nu_k|}|\zeta-\nu_k|\right]\right)\\
&= -\log 2+2\log(\alpha-\cos\theta_k)+\log|\wp(-\mathrm{i}\log\nu_k)+C|^2\\
&\qquad -\frac{1}{2}\lim_{\zeta\to\nu_k}\log\left|\frac{\nu_k(\wp'(-\mathrm{i}\log\zeta)-\wp'(-\mathrm{i}\log\nu_k))}{\zeta-\nu_k}\right|^2\\
&= -\log 2+2\log(\alpha-\cos\theta_k)+\log|\wp(-\mathrm{i}\log\nu_k)+C|^2-\frac{1}{2}\log\left|\wp''(-\mathrm{i}\log\nu_k)\right|^2.
\end{aligned}$$

We can see that the stationary condition is satisfied:

$$\nu_k\frac{\partial}{\partial\nu_k}\widetilde{\psi}_\infty(\nu_k,\overline{\nu}_k)=-\sin\theta_k-\mathrm{i}\frac{\wp'(-\mathrm{i}\log\nu_k)}{\wp(-\mathrm{i}\log\nu_k)+C}+\frac{\mathrm{i}}{2}\frac{\wp'''(-\mathrm{i}\log\nu_k)}{\wp''(-\mathrm{i}\log\nu_k)}=0,$$

using (A2) and $\theta_k=0$ or $\pi$ for $k=1,2,3$. Second, for the point vortex with the strength $\Gamma_0=+2\pi$ at $\zeta=\nu_0=1$, we have (again with $m=1$)

$$\begin{aligned}
\widetilde{\psi}_\infty(\nu_0,\overline{\nu}_0) &= \lim_{\zeta\to\nu_0}\left(-\frac{1}{2}\log\left[\frac{4}{(\alpha-\cos\theta)^2}\frac{|\wp'(-\mathrm{i}\log\zeta)|^2}{|\wp(-\mathrm{i}\log\zeta)+C|^4}\right]+\log\left[\frac{(\alpha-\cos\theta_0)}{|\nu_0|}|\zeta-\nu_0|\right]\right)\\
&= -\log 2+2\log(\alpha-\cos\theta_0)-\frac{1}{2}\lim_{\zeta\to\nu_0}\log\left|\frac{\nu_0\wp'(-\mathrm{i}\log\zeta)}{(\zeta-\nu_0)(\wp(-\mathrm{i}\log\zeta)+C)^2}\right|^2\\
&= -2\log 2+2\log(\alpha-\cos\theta_0),
\end{aligned}$$

since using (A3) and (A4) we find

$$\lim_{\zeta\to\nu_0}\log\left|\frac{\nu_0\wp'(-\mathrm{i}\log\zeta)}{(\zeta-\nu_0)(\wp(-\mathrm{i}\log\zeta)+C)^2}\right|^2=\lim_{\zeta\to\nu_0}\log\left|\left(\frac{2\mathrm{i}\log(\zeta/\nu_0)}{\zeta/\nu_0-1}\right)^2(1+o(-\mathrm{i}\log\zeta))\right|=\log 4.$$

From this, we find that the stationary condition is satisfied: $\nu_0\frac{\partial}{\partial\nu_0}\widetilde{\psi}_\infty(\nu_0,\overline{\nu}_0)=-\sin\theta_0=0$.

Lastly, the point vortices at $\zeta=\widehat{\nu}_k=\exp(\mathrm{i}\widehat{\omega}_k)$ with $\wp(\widehat{\omega}_k)+C=0$ and $|\widehat{\nu}_k|=\exp(r_c(\widehat{\theta}_k))$ have the same strength $\widehat{\Gamma}_k=-4\pi$ for $k=1,2$. The modified stream function (23) in this case is given by (with $m=-2$)

$$\begin{aligned}\widetilde{\psi}_\infty(\widehat{v}_k,\overline{\widehat{v}}_k) &= \lim_{\zeta\to\widehat{v}_k}\left(-\frac{1}{2}\log\left[\frac{4}{(\alpha-\cos\widehat{\theta}_k)^2}\frac{|\wp'(-\mathrm{i}\log\zeta)|^2}{|\wp(-\mathrm{i}\log\zeta)+C|^4}\right]-2\log\left[\frac{(\alpha-\cos\widehat{\theta}_k)}{|\widehat{v}_k|}|\zeta-\widehat{v}_k|\right]\right)\\ &= -\log 2-\log(\alpha-\cos\widehat{\theta}_k)-\log|\wp'(-\mathrm{i}\log\widehat{v}_k)|+\lim_{\zeta\to\widehat{v}_k}\log\left|\frac{\widehat{v}_k(\wp(-\mathrm{i}\log\zeta)+C)}{\zeta-\widehat{v}_k}\right|^2\\ &= -\log 2-\log(\alpha-\cos\widehat{\theta}_k)+\log|\wp'(-\mathrm{i}\log\widehat{v}_k)|.\end{aligned}$$

Here we have used

$$\begin{aligned}\lim_{\zeta\to\widehat{v}_k}\log\left|\frac{\widehat{v}_k(\wp(-\mathrm{i}\log\zeta)+C)}{\zeta-\widehat{v}_k}\right|^2 &= \lim_{\zeta\to\widehat{v}_k}\log\left|\frac{\widehat{v}_k(\wp(-\mathrm{i}\log\zeta)-\wp(-\mathrm{i}\log\widehat{v}_k))}{\zeta-\widehat{v}_k}\right|^2\\ &= \log|\wp'(-\mathrm{i}\log\widehat{v}_k)|^2.\end{aligned}$$

Hence, the stationary condition is reduced to

$$H(\widehat{v}_k)\equiv\widehat{v}_k\frac{\partial}{\partial\widehat{v}_k}\widetilde{\psi}_\infty(\widehat{v}_k,\overline{\widehat{v}}_k)=\frac{\sin\widehat{\theta}_k}{2}-\frac{\mathrm{i}}{2}\frac{\wp''(-\mathrm{i}\log\widehat{v}_k)}{\wp'(-\mathrm{i}\log\widehat{v}_k)}=0,\qquad k=1,2.$$

Let us now suppose that $C$ is real. Since $\wp$ is even, i.e., $\wp(z)=\wp(-z)$, it follows that $0=\wp(\widehat{\omega}_1)+C=\wp(-\widehat{\omega}_1)+C$, and so $\widehat{\omega}_2=-\widehat{\omega}_1$. We then have $H(\widehat{v}_1)=-H(\widehat{v}_2)$ since using $\widehat{\omega}_2=-\widehat{\omega}_1$ we first get

$$\wp'(\widehat{\omega}_2)=\wp'(-\widehat{\omega}_1)=-\wp'(\widehat{\omega}_1)\quad\Longrightarrow\quad\wp''(\widehat{\omega}_2)=\wp''(-\widehat{\omega}_1)=\wp''(\widehat{\omega}_1),$$

and also $\widehat{\theta}_2=2\pi-\widehat{\theta}_1$. It is thus sufficient to confirm that $H(\widehat{v}_1)=0$. We first show that $\widehat{\theta}_1=\pi$. The double periodicity of $\wp(z)$ gives a formula for $\widehat{\omega}_2$:

$$\wp(\widehat{\omega}_2)=\wp(-\widehat{\omega}_1)=\wp(2\omega_1+2\omega_3-\widehat{\omega}_1)\quad\Longrightarrow\quad\widehat{\omega}_2=2\omega_1+2\omega_3-\widehat{\omega}_1\in D_z,\tag{46}$$

for $\widehat{\omega}_1\in D_z$. The series expansion for $\wp(\omega_1+z)$ near $z=0$ is given by

$$\wp(\omega_1+z)=\wp(\omega_1)+\frac{z^2}{2}\wp''(\omega_1)+\frac{z^4}{4!}\wp^{(4)}(\omega_1)+\cdots$$

where the odd derivative terms must be zero because of the $z\mapsto -z$ symmetry $\wp(\omega_1+z)=\wp(-\omega_1-z)=\wp(2\omega_1-\omega_1-z)=\wp(\omega_1-z)$. In addition, since all the even derivatives $\wp^{(2k)}(\omega_1)$ are real, we have $\wp(\omega_1-\bar{z})=\overline{\wp(\omega_1+z)}$. Choosing the point $\bar{z}=\omega_1-\widehat{\omega}_1$, we obtain another formula for $\widehat{\omega}_2$:

$$0=\wp(\widehat{\omega}_1)+C=\overline{\wp(2\omega_1-\overline{\widehat{\omega}_1})}+C=\overline{\wp(2\omega_1-\overline{\widehat{\omega}_1})+C}\quad\Longrightarrow\quad\widehat{\omega}_2=2\omega_1-\overline{\widehat{\omega}_1}.\tag{47}$$

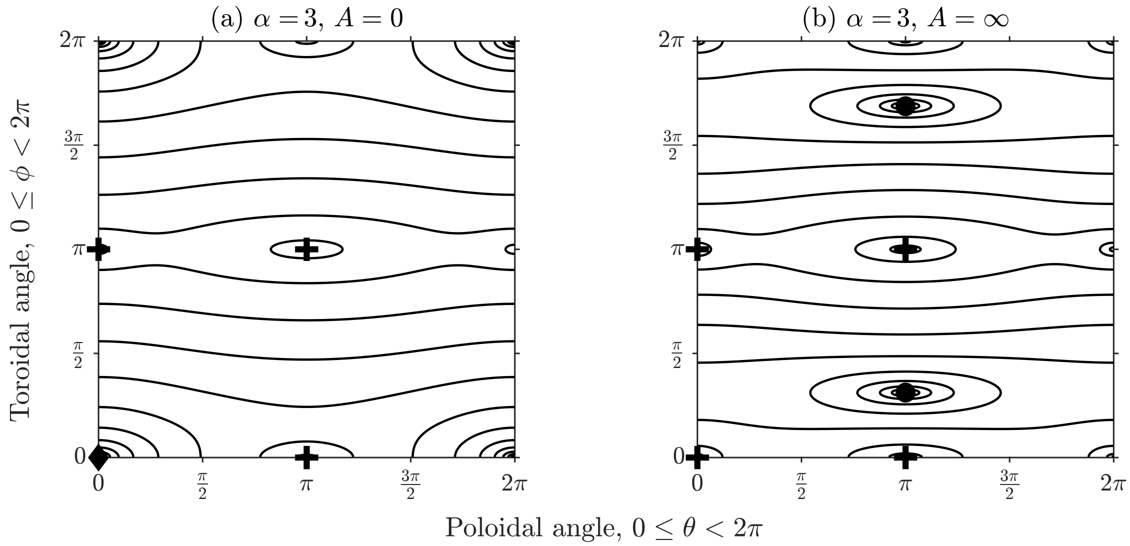


FIG. 7. Streamline contour plots with embedded point vortices (+,♦,●) with inhomogeneous strengths in (a) the $A = 0$ limit (44) and (b) the $A = \infty$ limit (45).

Equating the two formulas (46) and (47) for $\widehat{\omega}_2$ we obtain $2\omega_1 - \overline{\widehat{\omega}_1} = 2\omega_1 + 2\omega_3 - \widehat{\omega}_1$, which reduces to $\operatorname{Im}\widehat{\omega}_1 = -\mathrm{i}\omega_3 = -\frac{1}{2}\log\rho$. It follows from $\operatorname{Im}\widehat{\omega}_1 = -r_c(\widehat{\theta}_1) = -\log\sqrt{\rho}$ that $\widehat{\theta}_1 = \pi$. For the second term in $H(\widehat{v}_1)$, we use the formula (A5) and $\wp(\widehat{\omega}_1) + C = 0$ to get

$$|\wp'(\widehat{\omega}_k)|^2 = |4(C+e_1)(C+e_2)(C+e_3)| \neq 0 \quad \text{and} \quad \wp''(\widehat{\omega}_1) = -6C - \frac{1}{2}(e_1^2+e_2^2+e_3^2).$$

Accordingly, if we choose $C = -\frac{1}{12}(e_1^2+e_2^2+e_3^2)$, then $\wp''(\widehat{\omega}_1) = 0$, and we get a stationary solution.

Figure 7 shows the streamline patterns in the two limiting cases. The vorticity in the limiting case $A = 0$ (panel (a)) consists of three positive point vortices (+) with circulations $+2\pi$ each, together with one negative point vortex (♦) with circulation $-6\pi$, so that the total circulation is zero. In the limiting case $A = \infty$ (panel (b)) there are four point vortices (+) with circulations $+2\pi$ each and two negative vortices (●) with circulations $-4\pi$ each. The limiting solutions in both panels (a) and (b) thus contain point vortices of inhomogeneous strengths. The locations of the negative point vortices in panel (b) show rotational asymmetry in the toroidal direction. The background vorticity is due solely to the curvature term $\kappa(\mathbb{T}_\alpha)$ and does not contribute to the total circulation. This background vorticity is not shown in the figure.

### B. Loxodromic function

We can also obtain limiting solutions by substituting loxodromic functions for $h(\zeta)$ in (39) and (40). Taking $h(\zeta) = K(\zeta/a, \sqrt{\rho}) - K(\zeta/b, \sqrt{\rho})$ for $a, b \in D_\zeta$ in (39), the limiting solution $\psi_0$ is

$$\psi_0(\zeta, \overline{\zeta}) = -\frac{1}{2}\log\left[\frac{4|L(\zeta/a, \sqrt{\rho}) - L(\zeta/b, \sqrt{\rho})|^2}{(\alpha - \cos\theta)^2}\right]. \tag{48}$$

The four solutions of $L(\zeta/a, \sqrt{\rho}) - L(\zeta/b, \sqrt{\rho}) = 0$ are $\zeta = \nu_k = \pm\sqrt{ab}, \pm\sqrt{ab/\rho}$, $k = 1, 2, 3, 4$ (see §IV A), so that there are four point vortices at these points, each with strength $+2\pi$. In addition, it follows from (B9) that the function $L(\zeta/a, \sqrt{\rho}) - L(\zeta/b, \sqrt{\rho})$ has double poles at $\zeta = a$ and $\zeta = b$. Hence, the stream function (48) also contains two point vortices at $\zeta = a, b$, each with strength $-4\pi$, and the total circulation of these six point vortices therefore vanishes. That is to say, the Gauss condition (43) is satisfied.

We confirm the stationary condition separately for the point vortices at $\zeta = \nu_k$ and at $\zeta = a, b$. For the four point vortices with strength $+2\pi$ at $\zeta = \nu_k$, $k = 1, 2, 3, 4$, the modified stream function is (using $m = 1$ in (23))

$$\begin{aligned}\widetilde{\psi}_0(\nu_k, \overline{\nu}_k) &= \lim_{\zeta \to \nu_k}\left(-\frac{1}{2}\log\left[\frac{4|L(\zeta/a, \sqrt{\rho}) - L(\zeta/b, \sqrt{\rho})|^2}{(\alpha - \cos\theta)^2}\right] + \log\left[\frac{(\alpha - \cos\theta_k)}{|\nu_k|}|\zeta - \nu_k|\right]\right)\\ &= -\log 2 + 2\log(\alpha - \cos\theta_k) - \frac{1}{2}\log|M(\nu_k/a, \sqrt{\rho}) - M(\nu_k/b, \sqrt{\rho})|^2,\end{aligned}$$

where $r_c(\theta_k) = \log|\nu_k|$. We thus have the stationary condition

$$\nu_k \frac{\partial}{\partial \nu_k}\widetilde{\psi}_0(\nu_k, \overline{\nu}_k) = -\sin\theta_k - \frac{1}{2}\frac{N(\nu_k/a, \sqrt{\rho}) - N(\nu_k/b, \sqrt{\rho})}{M(\nu_k/a, \sqrt{\rho}) - M(\nu_k/b, \sqrt{\rho})} = -\sin\theta_k = 0,$$

since the zeros $\nu_k$ also satisfy $N(\nu_k/a, \sqrt{\rho}) - N(\nu_k/b, \sqrt{\rho}) = 0$ due to (B10) and (B12). Hence, the stationary condition is reduced to $\theta_k = 0$ or $\pi$. For the point vortex at $\zeta = a$ with strength $-4\pi$, the modified stream function (23) is given by (taking $m = -2$)

$$\begin{aligned}\widetilde{\psi}_0(a, \overline{a}) &= \lim_{\zeta \to a}\left(-\frac{1}{2}\log\left[\frac{4|L(\zeta/a, \sqrt{\rho}) - L(\zeta/b, \sqrt{\rho})|^2}{(\alpha - \cos\theta)^2}\right] - 2\log\left[\frac{(\alpha - \cos\theta_a)}{|a|}|\zeta - a|\right]\right)\\ &= -\log 2 - \log(\alpha - \cos\theta_a) + 2\log|a| - \lim_{\zeta \to a}\log|(\zeta - a)^2(L(\zeta/a, \sqrt{\rho}) - L(\zeta/b, \sqrt{\rho}))|\\ &= -\log 2 - \log(\alpha - \cos\theta_a).\end{aligned}$$

Here $\log|a| = r_c(\theta_a)$, and we have used $(\zeta - a)^2(L(\zeta/a, \sqrt{\rho}) - L(\zeta/b, \sqrt{\rho})) \to -a^2$ as $\zeta \to a$, which follows from (B9). Hence, we get the stationary condition

$$a\frac{\partial}{\partial a}\widetilde{\psi}_0(a, \overline{a}) = \frac{1}{2}\sin\theta_a = 0,$$

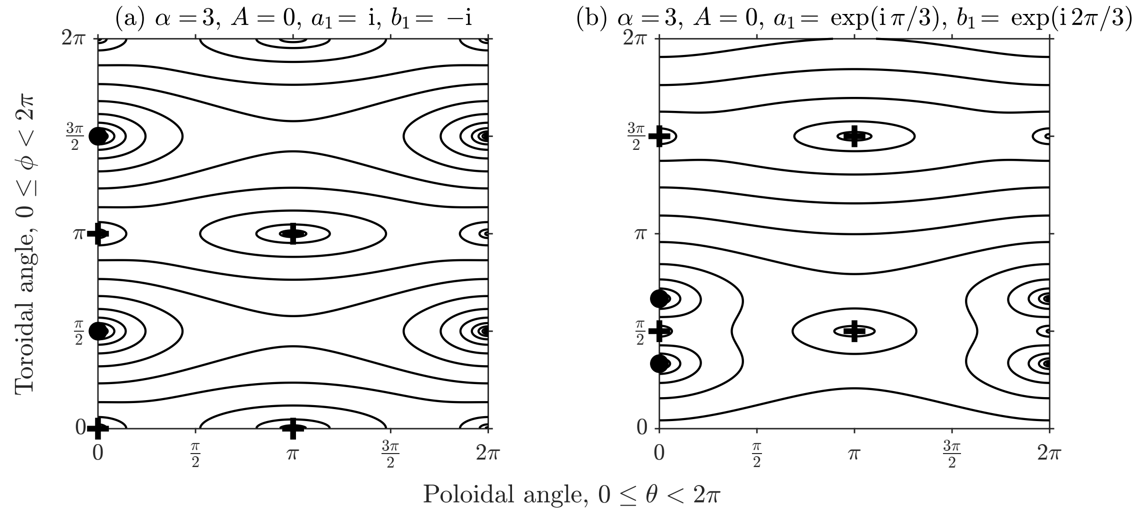


FIG. 8. Streamline contour plots with embedded point vortices (+,●) for the limiting stream function (48).

which shows that $\theta_a = 0$ or $\pi$. In the same way, we can also show that for the point vortex at $b$, we must have $\theta_b = 0$ or $\pi$ ($\theta_b$ is defined by $\log|b| = r_c(\theta_b)$).

Thus, in order for the stream function to be a steady solution, we need all six point vortices to be on the circles $|\zeta| = 1$ or $\sqrt{\rho}$. If we choose $|a| = |b| = 1$ or $|a| = |b| = \sqrt{\rho}$, then we also have $|v_k| = 1$ or $\sqrt{\rho}$ and the necessary conditions for the vortices to be stationary are satisfied. An example is the choice $a = \mathrm{i}$, $b = -\mathrm{i}$ which leads to $v_1 = 1$, $v_2 = -1$, $v_3 = \sqrt{\rho}$ and $v_4 = -\sqrt{\rho}$. Note that the situation for the stream function $\psi_0$ is somewhat different from the case of $\hat{n} = 1$ discussed in §IV A, as the point vortex stationary conditions impose further conditions on $a$ and $b$.

Figure 8 shows example solutions in the limit $A = 0$. In (a) we choose $a_1 = \mathrm{i}$ and $b_1 = -\mathrm{i}$ and in (b) we choose $a_1 = \mathrm{e}^{\mathrm{i}\,\pi/3}$ and $b_1 = \mathrm{e}^{\mathrm{i}\,2\pi/3}$. There are four positive point vortices (+) with circulations $+2\pi$ each and two negative point vortices (●) of circulations $-4\pi$ each, so that the total circulation is zero. Only the curvature term contributes to the background vorticity and is not shown in the figure.

We now turn to a description of the other limiting solution $\psi_\infty$ given by (40). Taking $h(\zeta) = K(\zeta/a, \sqrt{\rho}) - K(\zeta/b, \sqrt{\rho})$ for $a, b \in D_\zeta$ with $a \neq b$, we get

$$\psi_\infty(\zeta, \overline{\zeta}) = -\frac{1}{2}\log\left[\frac{4}{(\alpha - \cos\theta)^2}\frac{|L(\zeta/a, \sqrt{\rho}) - L(\zeta/b, \sqrt{\rho})|^2}{|K(\zeta/a, \sqrt{\rho}) - K(\zeta/b, \sqrt{\rho}) + C|^4}\right]. \tag{49}$$

The stream function $\psi_\infty$ contains point vortices with strength $+2\pi$ at the four zeros $v_k = \pm\sqrt{ab}$, $\pm\sqrt{ab/\rho}$ of $L(\zeta/a, \sqrt{\rho}) - L(\zeta/b, \sqrt{\rho})$, $k = 1, 2, 3, 4$. It also contains two point vortices with strength $-4\pi$ at the two zeros, say $\widehat{v}_k$, $k = 1, 2$, of $h(\zeta) + C$. Note that the poles of $h(\zeta)$, at

$\zeta = a, b$, are removable. Since the total circulation vanishes, the Gauss condition (21) is satisfied

Turning to the stationary condition for the six point vortices, we first consider the four point vortices with strength $+2\pi$ at $\nu_k$, $k = 1,2,3,4$. The modified stream function (23) is given by (with $m = 1$)

$$\begin{aligned}\widetilde{\psi}_\infty(\nu_k, \overline{\nu}_k) = & \lim_{\zeta\to\nu_k}\left(-\frac{1}{2}\log\left[\frac{4}{(\alpha-\cos\theta)^2}\frac{|L(\zeta/a,\sqrt{\rho})-L(\zeta/b,\sqrt{\rho})|^2}{|K(\zeta/a,\sqrt{\rho})-K(\zeta/b,\sqrt{\rho})+C|^4}\right]\right.\\ & \left. +\log\frac{(\alpha-\cos\theta_k)}{|\nu_k|}|\zeta-\nu_k|\right)\\ = & -\log 2 + 2\log(\alpha-\cos\theta_k) + \log|K(\nu_k/a,\sqrt{\rho})-K(\nu_k/b,\sqrt{\rho})+C|^2\\ & -\frac{1}{2}\log|M(\nu_k/a,\sqrt{\rho})-M(\nu_k/b,\sqrt{\rho})|^2,\end{aligned}$$

where $r_c(\theta_k) = \log|\nu_k|$. Hence, the stationary condition is given by

$$\begin{aligned}\nu_k\frac{\partial}{\partial\nu_k}\widetilde{\psi}_\infty(\nu_k,\overline{\nu}_k) = & -\sin\theta_k + \frac{L(\nu_k/a,\sqrt{\rho})-L(\nu_k/b,\sqrt{\rho})}{K(\nu_k/a,\sqrt{\rho})-K(\nu_k/b,\sqrt{\rho})+C}\\ & -\frac{1}{2}\frac{N(\nu_k/a,\sqrt{\rho})-N(\nu_k/b,\sqrt{\rho})}{M(\nu_k/a,\sqrt{\rho})-M(\nu_k/b,\sqrt{\rho})}\\ = & -\sin\theta_k = 0,\end{aligned}$$

where we have used (B10) and (B12). The stationary condition is once again reduced to $\theta_k = 0$ or $\pi$, which is equivalent to $|\nu_k| = 1$ or $\sqrt{\rho}$.

Next, for the point vortices with strength $-4\pi$ at the zeros $\zeta = \widehat{\nu}_k$ satisfying

$$h(\zeta)+C = K(\widehat{\nu}_k/a,\sqrt{\rho})-K(\widehat{\nu}_k/b,\sqrt{\rho})+C = 0, \tag{50}$$

we have (using $m = -2$ in (23))

$$\begin{aligned}\widetilde{\psi}_\infty(\widehat{\nu}_k,\overline{\widehat{\nu}}_k) = & \lim_{\zeta\to\widehat{\nu}_k}\left(-\frac{1}{2}\log\left[\frac{4}{(\alpha-\cos\theta)^2}\frac{|L(\zeta/a,\sqrt{\rho})-L(\zeta/b,\sqrt{\rho})|^2}{|K(\zeta/a,\sqrt{\rho})-K(\zeta/b,\sqrt{\rho})+C|^4}\right]\right.\\ & \left. -2\log\frac{(\alpha-\cos\widehat{\theta}_k)}{|\widehat{\nu}_k|}|\zeta-\widehat{\nu}_k|\right)\\ = & -\log 2 - \log(\alpha-\cos\widehat{\theta}_k) + \frac{1}{2}\log|L(\widehat{\nu}_k/a,\sqrt{\rho})-L(\widehat{\nu}_k/b,\sqrt{\rho})|^2,\end{aligned}$$

where $\log|\widehat{\nu}_k| = r_c(\widehat{\theta}_k)$. This gives rise to the following stationary condition,

$$\widehat{\nu}_k\frac{\partial}{\partial\widehat{\nu}_k}\widetilde{\psi}_\infty(\widehat{\nu}_k,\overline{\widehat{\nu}}_k) = \frac{1}{2}\sin\widehat{\theta}_k + \frac{1}{2}\frac{M(\widehat{\nu}_k/a,\sqrt{\rho})-M(\widehat{\nu}_k/b,\sqrt{\rho})}{L(\widehat{\nu}_k/a,\sqrt{\rho})-L(\widehat{\nu}_k/b,\sqrt{\rho})}.$$

Hence, we need to check if

$$\sin\widehat{\theta}_k + \frac{M(\widehat{\nu}_k/a,\sqrt{\rho})-M(\widehat{\nu}_k/b,\sqrt{\rho})}{L(\widehat{\nu}_k/a,\sqrt{\rho})-L(\widehat{\nu}_k/b,\sqrt{\rho})} = 0 \tag{51}$$

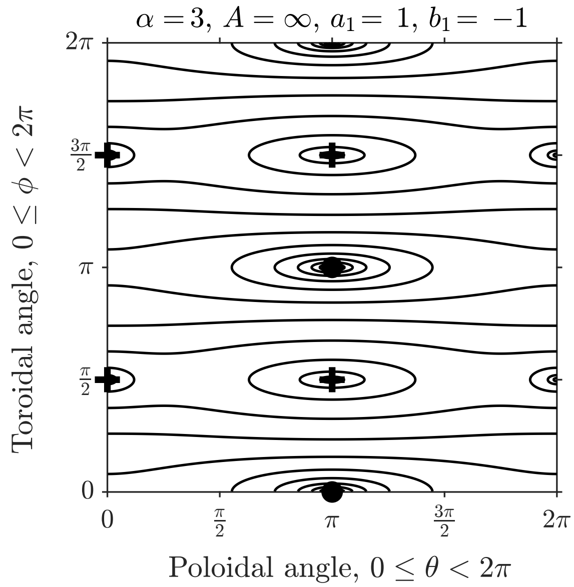


FIG. 9. Streamline contour plots for the limiting stream function (49). In this case there are four point vortices with circulations $+2\pi$ each (+), and two point vortices with circulations $-4\pi$ each (●) making the total circulation zero. The background vorticity due to $\kappa(\mathbb{T}_\alpha)$ is not shown.

for given $a$, $b$ and $C$.

When we take $a = 1$, $b = -1$ and $C = 0$ for instance, we have six point vortices at $v_k = \pm\mathrm{i}$, $\pm\mathrm{i}\sqrt{\rho}$ and $\widehat{v}_k = \pm\sqrt{\rho}$. The zeros $\widehat{v}_k$ can be obtained by noting that $K(\pm\sqrt{\rho}, \sqrt{\rho}) = 0$ due to (B3). Since $|ab| = 1$, the point vortices at $v_k$ with strengths $+2\pi$ are stationary. The point vortices at $\widehat{v}_k$ with the strength $-4\pi$ satisfy (51), since $\widehat{\theta}_k = \pi$ and $M(\pm\sqrt{\rho}, \sqrt{\rho}) = 0$ due to (B11). This example is shown in figure 9. Note that it is not easy to obtain point vortex equilibria for other choices of $a$, $b$ and $C$, since (50) and (51) give rise to three complex equations for two complex numbers, which is over-determined in general.

## VI. SUMMARY AND DISCUSSION

We have constructed a class of vortex solutions to the modified Liouville equation (5) on the surface of a curved torus, in which point vortices are in equilibrium with a fixed background vorticity. The non-trivial part of the background vorticity is exponentially related to the stream function, and this allows us to construct stationary point vortex configurations with the strengths of the embedded point vortices being quantized. The Liouville solutions are regarded as equilibria of the point-vortex system (22) in the sense of the one-way interaction model discussed in §I. They are not stationary solutions to the incompressible Euler equation, since the background Liouville-type vorticity (5) is not a functional of the stream function $\psi$. This is in contrast to the solutions of the Liouville-type equation in the plane (Krishnamurthy *et al.*, 2019) and on the sphere (Crowdy, 2004) providing steady solutions of the Euler equation.

Various solutions can be constructed by making different choices for the analytic function in the Liouville solution (15). We have chosen such functions in terms of the Weierstrass $\wp$-function and in terms of the Schottky–Klein prime function on an annulus. We also find limiting solutions in which the background Liouville-type vorticity can be turned off, leaving a set of quantized point vortices in equilibrium with only the background vorticity due to the curvature of the torus. The examples discussed show several interesting features of the solutions. The point vortex strengths are all equal and of the same sign for solutions containing both point vortices and the background Liouville-type vorticity. There are also regions of concentrated but smooth vorticity, which can move around smoothly as some parameter is varied, while the point vortex positions are independent of the parameter. In the limiting cases, we get point vortices with quantized but inhomogeneous strengths with some of the solutions lacking rotational symmetry. We find that the curvature of the torus restricts the poloidal locations of the point vortices to the innermost ($\theta = 0$) and outermost ($\theta = \pi$) circles of the torus. This restriction originating from the curvature shows up in the point vortex stationary condition as the $\sin\theta$ term, for example in (35).

In the planar case, point vortex equilibria with no background vorticity have been shown to be closely related to the Liouville-type equation (3) (Krishnamurthy *et al.*, 2020). These 'pure' point vortex equilibria were obtained as limiting solutions. The limiting solutions that we find in §V result in quantized point vortex equilibria on the torus, but embedded in background vorticity due to the curvature of the torus. More general families of solutions called "Liouville chains" have been found in the planar case (Krishnamurthy *et al.*, 2021), finding such iterated solutions on the torus is an open problem. One important difference between the planar case and the torus is the absence of the Gauss condition in the former. We can also consider the problem on other manifolds such as a sphere. Since the Euler characteristic of a sphere is non-zero, the curvature term affects the Gauss condition differently. The point vortex stationary condition is however simpler in the case of a sphere due to its constant curvature.

A two-way interaction model has been considered by Newton and Sakajo (2007) in the numerical computation of point vortices embedded in a continuous background vorticity corresponding to solid body rotation on a sphere. They discretize the background vorticity distribution into a collection of strips of constant vorticity and tracked the evolutions of these strips and the point vortices simultaneously. For the case of an intially rigidly rotating ring of point vortices embedded in the background, they observe the formation of Rossby waves in the solution, which destroy the ring structure of the point vortex equilibria.

We can consider a similar two-way interaction model on the torus with a set of quantized point vortices embedded in a Liouville-type background vorticity distribution. It must be noted here that numerical solution of the Euler equation on a torus is itself a challenging problem. Since the two-way interaction model is a useful discretization of Euler flow on a rotating sphere (Newton and Sakajo, 2007), it is interesting to ask whether such a model can be considered on the torus. The solutions obtained here can be used as computationally convenient initial vorticity distributions for a two-way interaction model on the surface of a torus. Such investigations will be reported in the future.


## ACKNOWLEDGMENTS

This work is supported by JSPS Kakenhi(B) #18H01136T, JSTMirai (#18076942), RIKEN iTHEMS program and the grant from the Simons Fellow for the programme in the Isaac Newton Institute. The authors would like to thank Professor Darren Crowdy for discussion. The authors would also like to thank the Isaac Newton Institute for Mathematical Sciences for support and hospitality during the programme [CAT] when work on this paper was undertaken. This work was supported by: EPSRC grant number EP/R014604/1. The authors are grateful to the anonymous referee for helpful comments which led to an improved paper.


## DATA AVAILABILITY STATEMENT

Data sharing is not applicable to this article as no new data were created or analyzed in this study.

## Appendix A: The Weierstrass $\wp$ function.

In this appendix, we provide a short review of the doubly periodic Weierstrass $\wp$ function using formulae provided in the handbook of Abramowitz and Stegun (1992). Consider the fundamental domain $D_z$, in a complex $z$-plane, over which $\wp(z)$ is defined:

$$D_z = \{z \in \mathbb{C} \,|\, 0 \leqq \mathrm{Re}(z) < 2\pi, -\log\rho < \mathrm{Im}(z) \leqq 0\}. \tag{A1}$$

Here $\rho \in \mathbb{R}$, $0 < \rho < 1$ is a parameter and the half periods of $\wp(z)$, $\omega_1$ and $\omega_3$, are given by $\omega_1 = \pi$ and $\omega_3 = -\frac{\mathrm{i}}{2}\log\rho$. We first note that the derivative of $|\wp(z)|$ is also doubly periodic, since $\wp'(z)^2 = (\wp(z) - e_1)(\wp(z) - e_2)(\wp(z) - e_3)$ for some constants $e_1, e_2, e_3 \in \mathbb{C}$. Second, $\wp(z)$ has a double pole at $z = 0 \equiv \omega_0$ and its derivative $\wp'(z)$ has three simple zeros, one each at the points of half periods $z = \omega_1$, $\omega_3$, and one at the center of the fundamental domain $z = \omega_2 = \omega_1 + \omega_3 = \pi - \frac{\mathrm{i}}{2}\log\rho$. The following useful formula shows that the third derivative $\wp'''(z)$ also vanishes at the points $\omega_k$:

$$\wp'''(\omega_k) = 12\wp(\omega_k)\wp'(\omega_k) = 0, \qquad k = 1, 2, 3. \tag{A2}$$

Finally, the $\wp$-function admits a Laurent series expansion in the neighborhood of the origin:

$$\wp(z) = \frac{1}{z^2} + c_2 z^2 + c_3 z^4 + \cdots = \frac{1}{z^2}(1 + o(z^3)), \quad z \to 0, \tag{A3}$$

for some non-zero constants $c_2$ and $c_4$. Thereby the derivative is represented by

$$\wp'(z) = -\frac{2}{z^3} + 2c_2 z + 4c_3 z^3 + \cdots = -\frac{2}{z^3}(1 + o(z^3)), \quad z \to 0. \tag{A4}$$

We have the standard definition $\wp(\omega_k) = e_k \in \mathbb{R}$, $k = 1, 2, 3$, with $e_1 > 0 > e_3$ and $e_1 > e_2 > e_3$. We recall the formulas

$$(\wp'(z))^2 = 4(\wp(z) - e_1)(\wp(z) - e_2)(\wp(z) - e_3), \qquad \wp''(z) = 6\wp(z) - \frac{1}{2}(e_1^2 + e_2^2 + e_3^2). \tag{A5}$$

## Appendix B: Schottky–Klein prime functions

The Schottky-Klein prime function is a special function defined on multiply-connected circular domains (Crowdy, 2020). The prime function defined on the annulus $D_\zeta = \{\zeta \in \mathbb{C} \,|\, \rho < |\zeta| \leqq 1\}$, is essentially the $P$-function given by the infinite product:

$$P(\zeta, \sqrt{\rho}) = (1 - \zeta)\prod_{k=1}^{\infty}(1 - \rho^k\zeta)(1 - \rho^k/\zeta). \tag{B1}$$

Note that $P(\zeta, \sqrt{\rho})$ has a simple zero in $D_\zeta$, at $\zeta = 1$. The $K$-function defined in terms of the logarithmic derivative of $P(\zeta, \sqrt{\rho})$ is

$$K(\zeta, \sqrt{\rho}) = \frac{\zeta P'(\zeta, \sqrt{\rho})}{P(\zeta, \sqrt{\rho})}. \tag{B2}$$

Here, the prime denotes derivatives with respect to the first argument, thus $P'(\zeta,\sqrt{\rho}) = \frac{\mathrm{d}P(\zeta,\sqrt{\rho})}{\mathrm{d}\zeta}$. It can be verified from these definitions that the $K$-function satisfies the useful identity

$$K(\rho\zeta,\sqrt{\rho}) = K(\zeta,\sqrt{\rho}) - 1 = -K(1/\zeta,\sqrt{\rho}). \tag{B3}$$

Further, we can deduce the infinite series formula

$$K(\zeta,\sqrt{\rho}) = \frac{\zeta}{\zeta-1} + \sum_{k=1}^{\infty}\left(\frac{-\rho^k\zeta}{1-\rho^k\zeta} + \frac{\rho^k/\zeta}{1-\rho^k/\zeta}\right) = \frac{1}{\zeta-1} + O(1) \quad \text{as } \zeta \to 1, \tag{B4}$$

showing that $K(\zeta,\sqrt{\rho})$ has a simple pole singularity at $\zeta = 1$.

We can define further functions via derivatives. The $L$, $M$, and $N$-functions are defined by

$$L(\zeta,\sqrt{\rho}) = \zeta K'(\zeta,\sqrt{\rho}), \tag{B5}$$

$$M(\zeta,\sqrt{\rho}) = \zeta L'(\zeta,\sqrt{\rho}), \tag{B6}$$

$$N(\zeta,\sqrt{\rho}) = \zeta M'(\zeta,\sqrt{\rho}). \tag{B7}$$

The infinite series expansion for the $L$-function can be worked out using (B4) and (B5) to be

$$L(\zeta,\sqrt{\rho}) = -\frac{\zeta}{(\zeta-1)^2} - \sum_{k=1}^{\infty}\left(\frac{\rho^k\zeta}{(1-\rho^k\zeta)^2} + \frac{\rho^k/\zeta}{(1-\rho^k/\zeta)^2}\right), \tag{B8}$$

showing that it has a double pole at $\zeta = 1$, since

$$L(\zeta,\sqrt{\rho}) = -\frac{1}{(\zeta-1)^2} - \frac{1}{\zeta-1} + O(1) \quad \text{as } \zeta \to 1. \tag{B9}$$

The following important properties of the $L$-function can be proven using (B8):

$$L(\zeta,\sqrt{\rho}) = L(\rho\zeta,\sqrt{\rho}) = L(1/\zeta,\sqrt{\rho}). \tag{B10}$$

The properties of the $M$-function can be found by taking derivatives of (B10). We find

$$M(\zeta,\sqrt{\rho}) = M(\rho\zeta,\sqrt{\rho}) = -M(1/\zeta,\sqrt{\rho}). \tag{B11}$$

Then from (B11), we can find the properties of the $N$-function:

$$N(\zeta,\sqrt{\rho}) = N(\rho\zeta,\sqrt{\rho}) = N(1/\zeta,\sqrt{\rho}). \tag{B12}$$

These properties show that the $L$, $M$ and $N$-functions are all loxodromic functions, i.e. they are unchanged under $\zeta \mapsto \rho\zeta$. Further, the $L$ and $N$-functions are unchanged under $\zeta \mapsto 1/\zeta$, whereas the $M$-function picks up a minus sign under this mapping.

We finally mention that for the purpose of numerical computations, the above special functions are all evaluated using a rapidly convergent Laurent series for the prime function in the annulus, see Crowdy (2010, 2020) for details.

## REFERENCES


Abo-Shaeer, J. R., Raman, C., Vogels, J. M., and Ketterle, W., "Observation of vortex lattices in Bose-Einstein condensates." Science **292**, 476–479 (2001).

Abramowitz, M. and Stegun, I. A., eds., *Handbook of mathematical functions with formulas, graphs, and mathematical tables* (Dover Publications, Inc., New York, 1992) pp. xiv+1046, reprint of the 1972 edition.

Abrikosov, A. A., "Nobel lecture: Type-II superconductors and the vortex lattice," Reviews of Modern Physics **76**, 975–979 (2004).

Akerblom, N., Cornelissen, G., Stavenga, G., and van Holten, J. W., "Nonrelativistic chern-simons vortices on the torus," Journal of Mathematical Physics **52**, 072901 (2011).

Aref, H., Newton, P. K., Stremler, M. A., Tokieda, T., and Vainchtein, D. L., "Vortex Crystals," (Elsevier, 2003) pp. 1–79.

Bhutani, O. P., Moussa, M. H. M., and Vijayakumar, K., "On the generalized forms of exact solutions to the Liouville equation via direct approach," Internat. J. Engrg. Sci. **32**, 1965–1969 (1994).

Calogero, F. and Degasperis, A., *Spectral transform and solitons. Vol. I*, Studies in Mathematics and its Applications, Vol. 13 (North-Holland Publishing Co., Amsterdam-New York, 1982) pp. xv+516, tools to solve and investigate nonlinear evolution equations, Lecture Notes in Computer Science, 144.

Corrada-Emmanuel, A., "Exact solution for superfluid film vortices on a torus," Physical Review Letters **72**, 681–684 (1994).

Crowdy, D., "Polygonal N-vortex arrays: A Stuart model," Phys. Fluids **15**, 3710–3717 (2003).

Crowdy, D., "The schottky-klein prime function on the schottky double of planar domains," Computational Methods and Function Theory **10**, 501–517 (2010).

Crowdy, D., *Solving Problems in Multiply Connected Domains* (SIAM - Society for Industrial and Applied Mathematics, 2020) p. 434.

Crowdy, D. G., "General solutions to the 2D Liouville equation," Int. J. Eng. Sci. **35**, 141–149 (1997).

Crowdy, D. G., "Stuart vortices on a sphere," J. Fluid Mech. **498**, 381–402 (2004).

Engels, P., Coddington, I., Haljan, P. C., and Cornell, E. A., "Nonequilibrium effects of anisotropic compression applied to vortex lattices in bose-einstein condensates," Physical Review Letters **89**

(2002), 10.1103/physrevlett.89.100403.

Engels, P., Coddington, I., Haljan, P. C., Schweikhard, V., and Cornell, E. A., "Observation of long-lived vortex aggregates in rapidly rotating bose-einstein condensates," Physical Review Letters **90** (2003), 10.1103/physrevlett.90.170405.

Feynman, R., "Chapter II application of quantum mechanics to liquid helium," in *Progress in Low Temperature Physics* (Elsevier, 1955) pp. 17–53.

Green, C. C. and Marshall, J. S., "Green's function for the Laplace-Beltrami operator on a toroidal surface," Proc. R. Soc. Lond. Ser. A Math. Phys. Eng. Sci. **469**, 20120479, 18 (2013).

Horváthy, P. and Yéra, J.-C., Letters in Mathematical Physics **46**, 111–120 (1998).

Hurwitz, A. and Courant, R., *Vorlesungen über allgemeine Funktionentheorie und elliptische Funktionen* (Interscience Publishers, Inc., New York, 1944) pp. xii+534.

Kimura, Y., "Vortex motion on surfaces with constant curvature," Proceedings of the Royal Society of London. Series A: Mathematical, Physical and Engineering Sciences **455**, 245–259 (1999).

Krishnamurthy, V. S., Wheeler, M. H., Crowdy, D. G., and Constantin, A., "Steady point vortex pair in a field of stuart-type vorticity," Journal of Fluid Mechanics **874**, R1 (2019).

Krishnamurthy, V. S., Wheeler, M. H., Crowdy, D. G., and Constantin, A., "A transformation between stationary point vortex equilibria," Proceedings of the Royal Society A: Mathematical, Physical and Engineering Sciences **476**, 20200310 (2020).

Krishnamurthy, V. S., Wheeler, M. H., Crowdy, D. G., and Constantin, A., "Liouville chains: new hybrid vortex equilibria of the two-dimensional euler equation," Journal of Fluid Mechanics **921** (2021), 10.1017/jfm.2021.285.

Liouville, J., "Surléquation aux différenes partielles $\frac{d^2 \log \lambda}{du dv} \pm \frac{\lambda}{2a^2} = 0$," J. Math. Pures et Appl. **18**, 71–72 (1853).

Machta, J. and Guyer, R. A., "Superfluid films in porous media," Physical Review Letters **60**, 2054–2057 (1988).

Majda, A. J. and Bertozzi, A. L., *Vorticity and Incompressible Flow*, Cambridge Texts in Applied Mathematics (Cambridge University Press, 2001).

Newton, P. K., *The N-Vortex Problem: Analytical Techniques*, Applied Mathematical Sciences (Springer New York, 2001).

Newton, P. K. and Chamoun, G., "Vortex lattice theory: a particle interaction perspective," SIAM Rev. **51**, 501–542 (2009).

Newton, P. K. and Sakajo, T., "The n -vortex problem on a rotating sphere. III. ring configurations coupled to a background field," Proceedings of the Royal Society A: Mathematical, Physical and Engineering Sciences **463**, 961–977 (2007).

Newton, P. K. and Shokraneh, H., "The n -vortex problem on a rotating sphere. i multi-frequency configurations," Proceedings of the Royal Society A: Mathematical, Physical and Engineering Sciences **462**, 149–169 (2005).

Saffman, P. G., *Vortex dynamics* (Cambridge University Press, 1992).

Sakajo, T., "Exact solution to a Liouville equation with Stuart vortex distribution on the surface of a torus," Proc. R. Soc. A **475**, 20180666 (2019a).

Sakajo, T., "Vortex crystals on the surface of a torus," Philos. Trans. Roy. Soc. A **377**, 20180344, 17 (2019b).

Sakajo, T. and Shimizu, Y., "Point vortex interactions on a toroidal surface," Proc. A. **472**, 20160271, 24 (2016).

Stuart, J. T., "On finite amplitude oscillations in laminar mixing layers," J. Fluid Mech. **29**, 417–440 (1967).

Tur, A. and Yanovsky, V., "Point vortices with a rational necklace: New exact stationary solutions of the two-dimensional euler equation," Physics of Fluids **16**, 2877–2885 (2004).

Tur, A., Yanovsky, V., and Kulik, K., "Vortex structures with complex points singularities in two-dimensional Euler equations. New exact solutions," Physica D: Nonlinear Phenomena **240**, 1069–1079 (2011), arXiv:arXiv:1201.5271v1.

Turner, A. M., Vitelli, V., and Nelson, D. R., "Vortices on curved surfaces," Reviews of Modern Physics **82**, 1301–1348 (2010).

Yarmchuk, E. J., Gordon, M. J. V., and Packard, R. E., "Observation of stationary vortex arrays in rotating superfluid helium," Phys. Rev. Lett. **43**, 214–217 (1979).